HHS Public Access

Author manuscript

Neuroimage. Author manuscript; available in PMC 2022 July 08.

Published in final edited form as:

Neuroimage. 2022 July 01; 254: 119139. doi:10.1016/j.neuroimage.2022.119139.

Reward and loss incentives improve spatial working memory by shaping trial-by-trial posterior frontoparietal signals

Youngsun T. Cho[a,b,c,d,*], **Flora Moujaes**[a,1], **Charles H. Schleifer**[a], **Martina Starc**[e], **Jie Lisa Ji**[a], **Nicole Santamauro**[a], **Brendan Adkinson**[a], **Antonija Kolobaric**[a], **Morgan Flynn**[a], **John H. Krystal**[a,i], **John D. Murray**[a,d,f], **Grega Repovs**[e], **Alan Anticevic**[a,c,d,g,h,i,*]

[a]Yale University, Department of Psychiatry, 300 George Street, Suite 901, New Haven, CT, 06511, USA

[b]Yale University, Child Study Center, 230 South Frontage Road, New Haven, CT, 06519, USA

[c]Connecticut Mental Health Center, Clinical Neuroscience Research Unit, 34 Park Street, 3rd floor, New Haven, CT, 06519, USA

[d]Yale University, Interdepartmental Neuroscience Program, Yale University Neuroscience Program, P.O. Box 208074, New Haven, CT, 06520, USA

[e]University of Ljubljana, Department of Psychology,

[*]Corresponding authors. youngsun.cho@yale.edu (Y.T. Cho), alan.anticevic@yale.edu (A. Anticevic).

[1]Present Address: Flora Moujaes: Department of Psychiatry, Psychotherapy and Psychosomatics, University of Zurich, Zurich, Switzerland; Charles H. Schleifer: University of California Los Angeles School of Medicine, Los Angeles, CA 90095, USA; Antonija Kolobaric: Department of Psychiatry, University of Pittsburgh, Pittsburgh, PA 15261, USA; Morgan Flynn: Vanderbilt University School of Medicine, Nashville, TN 27232, USA

Credit authorship contribution statement

Youngsun T. Cho: Conceptualization, Methodology, Software, Formal analysis, Investigation, Writing – original draft, Writing – review & editing, Visualization, Data curation, Funding acquisition. **Flora Moujaes:** Visualization, Data curation, Formal analysis, Software. **Charles H. Schleifer:** Investigation, Data curation, Software. **Martina Starc:** Software, Conceptualization. **Jie Lisa Ji:** Methodology, Data curation. **Nicole Santamauro:** Investigation, Supervision, Project administration. **Brendan Adkinson:** Investigation. **Antonija Kolobaric:** Investigation. **Morgan Flynn:** Investigation. **John H. Krystal:** Conceptualization, Supervision, Writing – review & editing. **John D. Murray:** Conceptualization, Supervision, Writing – review & editing. **Grega Repovs:** Conceptualization, Supervision, Methodology, Software, Writing – review & editing. **Alan Anticevic:** Conceptualization, Methodology, Software, Investigation, Writing – original draft, Writing – review & editing, Visualization, Supervision, Resources, Data curation, Funding acquisition.

Declarations of Competing Interest

JLJ previously worked for Neumora Therapeutics (formerly Blackthorn Therapeutics). JHK reports having received consulting payments from AstraZeneca Pharmaceuticals, Biogen, Biomedisyn Corporation, Bionomics, Boehringer Ingelheim International, COMPASS Pathways, Concert Pharmaceuticals, Epiodyne, EpiVario, Heptares Therapeutics, Janssen Research & Development, Otsuka America Pharmaceutical, Perception Neuroscience Holdings, Spring Care, Sunovion Pharmaceuticals, Takeda Industries, and Taisho Pharmaceutical. He has served on advisory boards for Bioasis Technologies, Biohaven Pharmaceuticals, BioXcel Therapeutics, Cadent Therapeutics, Cerevel Therapeutics, EpiVario, Eisai, Lohocla Research Corporation, Neumora Therapeutics, Novartis Pharmaceuticals Corporation, and PsychoGenics. He is a co-sponsor of a patent for the intranasal administration of ketamine for the treatment of depression and for the treatment of suicide risk that was licensed by Janssen Pharmaceuticals; has a patent related to the use of riluzole to treat anxiety disorders that was licensed by Biohaven Pharmaceuticals; has stock or stock options in Biohaven Pharmaceuticals, Luc Therapeutics, Cadent Pharmaceuticals, Neumora Therapeutics, Terran Biosciences, Spring Healthcare, and Sage Pharmaceuticals. He serves on the Board of Directors of Inheris Pharmaceuticals. He receives compensation for serving as editor of the journal Biological Psychiatry. GR consults for and holds equity in Neumora Therapeutics, and Manifest Sciences. JDM serves on the Technology Advisory Board for Neumora Therapeutics and holds equity, is a co-founder of Manifest Sciences and consults for Gilgamesh Pharmaceuticals. AA serves on the Technology Advisory Board for Neumora Therapeutics and holds equity, is a co-founder of Manifest Sciences and consults for Gilgamesh Pharmaceuticals. All other authors have no disclosures.

Supplementary materials

Supplementary material associated with this article can be found, in the online version, at doi:10.1016/j.neuroimage.2022.119139.

[f]Yale University, Department of Physics, 217 Prospect Street, New Haven, CT, 06511, USA

[g]University of Zagreb, University Psychiatric Hospital Vrapce

[h]Yale University, Department of Psychology, Box 208205, New Haven, CT, 06520-8205, USA

[i]Yale University, NIAAA Center for Translational Neuroscience of Alcoholism, 34 Park Street, 3rd floor, New Haven, CT 06519 USA

Abstract

Integrating motivational signals with cognition is critical for goal-directed activities. The mechanisms that link neural changes with motivated working memory continue to be understood. Here, we tested how externally cued and non-cued (internally represented) reward and loss impact spatial working memory precision and neural circuits in human subjects using fMRI. We translated the classic delayed-response spatial working memory paradigm from non-human primate studies to take advantage of a continuous numeric measure of working memory precision, and the wealth of translational neuroscience yielded by these studies. Our results demonstrated that both cued and non-cued reward and loss improved spatial working memory precision. Visual association regions of the posterior prefrontal and parietal cortices, specifically the precentral sulcus (PCS) and intraparietal sulcus (IPS), had increased BOLD signal during incentivized spatial working memory. A subset of these regions had trial-by-trial increases in BOLD signal that were associated with better working memory precision, suggesting that these regions may be critical for linking neural signals with motivated working memory. In contrast, regions straddling executive networks, including areas in the dorsolateral prefrontal cortex, anterior parietal cortex and cerebellum displayed decreased BOLD signal during incentivized working memory. While reward and loss similarly impacted working memory processes, they dissociated during feedback when money won or avoided in loss was given based on working memory performance. During feedback, the trial-by-trial amount and valence of reward/loss received was dissociated amongst regions such as the ventral striatum, habenula and periaqueductal gray. Overall, this work suggests motivated spatial working memory is supported by complex sensory processes, and that the IPS and PCS in the posterior frontoparietal cortices may be key regions for integrating motivational signals with spatial working memory precision.

Keywords

cognition; motivation; working memory; reward; parietal cortex; prefrontal cortex

1. Introduction

The ability to activate behaviors in response to incentives is critical for all species. Motivational drive arises when external cues signaling forthcoming incentives integrate with internal states to affect downstream processes (Berridge et al., 2009; Berridge, 2012; Schultz, 2016). A large body of prior work has shown that cognition is sensitive to incentives (Aarts et al., 2011; Braver et al., 2014; Botvinick and Braver, 2015; Pessoa, 2017), and this interaction between motivation and cognition has important implications for complex processes such as learning and decision-making (Dixon and Christoff, 2012;

Collins et al., 2014, 2017; Honig et al., 2020; Park et al., 2021). The co-disruption of motivation and cognition in common psychiatric illnesses further underscores the links between these two, often separately studied, systems (Aarts et al., 2015; Anticevic et al., 2015; Cho et al., 2018; Grahek et al., 2019).

Working memory (WM) is a key 'building block' of cognition that is required for higher-order cognition, including problem solving and abstraction. Intact maintenance of mnemonic information is therefore critical for functioning, and a body of prior work has shown that incentives can enhance WM through improvements in precision and reaction time (Gilbert and Fiez, 2004; Beck et al., 2010; Jimura and Braver, 2010; Gong and Li, 2014; Klyszejko et al., 2014; Wallis et al., 2015; Thurm et al., 2018; Manga et al., 2020; Sandry and Ricker, 2020; Brissenden et al., 2021; Zhou et al., 2021), though not capacity (Zhang and Luck, 2011). A number of related mechanisms likely underlie these effects. Visual processing can shift as a result of reward-stimuli associations, possibly enhancing attentional priorities (Engelmann and Pessoa, 2007; Morey et al., 2011; Chelazzi et al., 2013; Klyszejko et al., 2014; Sandry and Ricker, 2020), thereby influencing the encoding of stimuli and, ultimately, downstream cognitive performance (Small et al., 2005; Serences, 2008; Geier et al., 2010; Chelazzi et al., 2013; Rothkirch and Sterzer, 2015). As modeled by van den Berg and colleagues, it may be that optimization between the distribution of cognitive resources and the amount of reward at stake leads to differentially encoded stimuli (van den Berg and Ma, 2018). Key reward-stimuli associations are likely cemented by closely tracking outcomes, as receiving incentives is highly salient when linked to an action (Zink et al., 2004). Ultimately, these mechanisms affect the strength of reward representation and the ability to keep in mind future rewards. The strength of reward representation is therefore critical for motivated behaviors—stimuli previously associated with reward can affect WM, but this effect weakens if the reward-stimuli association is not repeatedly reinforced (Infanti et al., 2015; Klink et al., 2017). In addition, while rewards can improve task performance, reward information that is irrelevant to a task can impede performance (Krebs et al., 2010, 2011). Collectively, prior work suggests that incentives can have a powerful effect on cognitive performance.

Human neuroimaging studies suggest that regions that support working memory and cognition also integrate motivation; therefore the same systems appear capable of supporting cognition and flexibly integrating motivational and other affective cues (Perlstein et al., 2002; Braver et al., 2009). This includes a distributed network of regions primarily localized to the frontal and parietal cortices, including the dorsolateral prefrontal cortex (dlPFC), the precentral sulcus (PCS), intraparietal sulcus (IPS), inferior frontal gyrus, and anterior cingulate cortex (ACC) (Pochon et al., 2002; Gilbert and Fiez, 2004; Taylor et al., 2004; Krawczyk et al., 2007; Longe et al., 2009; Beck et al., 2010; Jimura et al., 2010; Krawczyk and D'Esposito, 2013; Belayachi et al., 2015). These neuroimaging studies highlight brain regions that likely support motivated WM, and also raise questions about where in the brain motivated working memory performance and neural signals can be linked. Identifying the regions where neural signal changes can be linked to changes in WM performance may lead to a more specific understanding of which processes ultimately affect WM during motivated conditions and contribute to goal-directed behaviors. This fundamental gap remains, in part, because some neuroimaging studies have not demonstrated measurable change in

working memory performance under motivating conditions, though neural modulation has been observed (Pochon et al., 2002; Taylor et al., 2004; Belayachi et al., 2015). In other studies, the effect of motivation on working memory has been measured with respect to reaction time, leaving open questions about the neural effects of motivational changes on accuracy (Krawczyk et al., 2007; Beck et al., 2010; Jimura et al., 2010). In only a few human neuroimaging studies have incentives shown to improve working memory accuracy (Gilbert and Fiez, 2004; Longe et al., 2009), though in neither study were direct links between behavior and brain identified.

To begin to bridge this gap, we designed a motivated working memory task for functional magnetic resonance imaging (fMRI) with the goal of identifying neural systems that support motivated WM and associated changes in WM accuracy. We translated a well-studied spatial working memory (sWM) task from non-human primate work (Hikosaka and Wurtz, 1983; Funahashi et al., 1989) that has yielded a rich understanding of single neuron physiology, and has inspired related computational models (Compte et al., 2000; Durstewitz et al., 2000; Murray et al., 2012; Wimmer et al., 2014), thereby allowing for interpretive findings across species and levels of neural circuits. Work using this task and related tasks in non-human primates has found that neuronal firing in the PFC, but also parietal and visual cortices, critically support sWM during the delay epoch when mnemonic information is maintained (Fuster, 1973; Funahashi et al., 1989; Barash et al., 1991; Constantinidis and Steinmetz, 1996; Miller et al., 1996; Chafee and Goldman-Rakic, 1998; Bisley et al., 2004; Vijayraghavan et al., 2007; Woloszyn and Sheinberg, 2009; Steenrod et al., 2013; Lundqvist et al., 2016). Other studies in monkeys suggest that executive functions that originate from the PFC, such as attention, may modulate the sensory cortices responsible for supporting information representation (Petrides, 2000; Pasternak and Greenlee, 2005). This concerted neural activity may reflect the extensive connections across the fronto-parietal-visual system (Barbas and Mesulam, 1981; Cavada and Goldman-Rakic, 1991; Petrides and Pandya, 1999) that have been mapped in non-human primates, and are likely relevant in humans. Notably, human neuroimaging of this sWM task has also identified a fronto-parietal-visual system that supports sWM (Sweeney et al., 1996; Curtis et al., 2004; Geier et al., 2009; Jerde et al., 2012; Mackey et al., 2017; Rahmati et al., 2018), and these findings align with the broader neuroimaging literature on sWM (McCarthy et al., 1994, 1996; Courtney et al., 1998; Lawrence et al., 2018).

We adapted this sWM task to test the effect of incentives on sWM neural systems and link changes in sWM performance with changes in neural signal. This task uses a continuous measure of sWM accuracy, potentially allowing for a wider range of responses, and decreased floor/ceiling effects. We hypothesized that using this task would yield a measurable effect of motivation on sWM accuracy, and allow us to examine the brain for associated neural signals. Reward and loss incentives were included, as both can be motivating (Knutson et al., 2001; Kim et al., 2006). We presented incentives under cued and non-cued conditions to test the hypothesis that externally and internally represented incentives could elicit motivational drive and modulate sWM, as models of incentive motivation suggest that motivation arises from integrating both external cues and internal states (Berridge, 2009, 2012). The feedback phase, which was designed to award larger amounts of money for better sWM accuracy, was examined to provide validation for the

impact of incentives, and another link between changes in sWM accuracy and neural modulation. Overall, we found that both externally and internally represented incentives elicited motivational drive to improve sWM accuracy, and that trial-by-trial improvements in sWM accuracy were associated with increases in BOLD signal in visual association regions of the posterior frontal (PCS) and parietal (IPS) cortices. Outcomes were observed to be highly salient, and tracked by subcortical and cortical brain regions, including the ventral striatum, habenula and periaqueductal gray. Taken together, our work suggests that motivation recruits complex sensory processes through IPS and PCS engagement to improve sWM.

2. Methods and materials

2.1. Subjects

33 right-handed, fluent English-speaking young adults (12 females, 21 males, age = 23.3 +/− 4.6 y/o) were recruited with community advertisement. All participants tolerated an MRI, had no current or lifetime history of psychiatric illness or substance use disorders for themselves or immediate family, had no severe medical or neurological illnesses, and had no history of significant head injury. Procedures were approved by the Yale Institutional Review Board.

2.2. Task design

We used a slow, event-related design to examine motivational interactions with cognition (Mint-Cog: Motivational Interactions with Cognition). All trials had a similar design and were time-locked to the time repetition (TR). Each trial began with a colored target circle presented in one of 40 pseudo-randomized locations within two concentric rings (390 or 415 pixel radius). This appearance of the colored target circle was the start of the encoding epoch, and this target circle remained on-screen for 1.4 s (Fig. 1A, Supplemental Figure 1A). When this circle disappeared, the delay epoch began and subjects maintained the previously presented spatial position while continuing central fixation. The delay epoch lasted 9.8 s. Next, a gray circle linked to a joystick appeared, signaling the start of the probe phase. Participants were instructed to place the gray circle where they best remembered the colored circle had been. The probe phase had a duration of 2.8 s. Response accuracy was measured as the angular distance between the target location and response circle. Inter-trial intervals were 13.3 s and began after the probe phase ended or after feedback was given in cued incentive trials (see below). Each block had 20 trials, half of which pseudorandomly had a reminder for central fixation that required a button press when the fixation point briefly turned blue (0.7 s) during the delay epoch (button pressed in >90% of trials).

The task began with a block of 20 motor trials without working memory that served as a control for the neutral, baseline sWM trials. In these trials, participants were informed at the start of the block that they did not need to remember the location of the colored target circle. The colored (yellow) circle re-appeared during the probe epoch, and subjects moved the probe as closely as possible to the target. After this, a block of 20 neutral sWM trials (yellow target circle) were presented. In this set of trials, participants were instructed at the

start of the block to remember the location of the initially presented yellow target circle, and the trial occurred as described earlier (encoding, delay, probe, ITI).

Participants were then instructed that they would be given $20 with the possibility for further gain or loss in upcoming trials depending on their ability to remember the location of the colored target circles. Four incentive blocks were presented and the presentation was counterbalanced across participants. Two of the blocks contained cued incentive trials. In these trials, the possibility for gain or loss was cued at the start of each trial by the color of the target circle, and participants were informed this at the start of each block. Across these two blocks there were a total of 16 cued reward trials (green target), and 16 cued loss trials (red target), with 8 neutral 'catch' trials (yellow target) interspersed to separate the incentivized trials. These trials were pseudorandomly presented across the two blocks. After each trial, feedback was given on the amount of money won or lost, and the running total. Two other blocks had non-cued incentive presentations. In the non-cued reward block, subjects were informed at the start of the block that they could win money on each trial but would not be given further reminders or feedback. In the non-cued loss block they were given instructions at the start of the block that they could lose money on each trial but that they would not be given any further reminders or feedback. Both non-cued incentive blocks appeared visually identical to neutral trials and the target circle was yellow to avoid cueing the possibility for incentive, and avoid association with a new color (Cho et al., 2018). The only feedback given was the monetary total at the end of each non-cued reward or loss block.

Incentive delivery was designed such that better performance resulted in more money won or less money lost. Thresholds for receiving reward or avoiding loss were individualized based on each participant's baseline neutral sWM performance. The participant's sWM performance for each trial during the sWM block was sorted from best to worst, and reward/loss thresholds were set according to this sorted list. For reward trials, $2 was awarded for performance in the top 40% of baseline sWM performances, $1.50 if between the top 41–50%, $1 if between the top 51–65%, and $0.50 if between the top 65–80%. For loss trials, no money was lost for performance in the top 40% of baseline sWM performances, $0.50 was lost if between the top 41–50% of trials, $1 if between the top 51–65% of trials, $1.50 if between the top 65–80% of trials, and $2 if in the bottom 20% of trials. The amount of money that could be won or lost on each trial was the same for the cued and non-cued incentive trials. The final total at the end of the task was paid to participants (mean $33.42 (standard dev = $16.03), and the range of money won was −$4.50−$69).

The task was presented on a Dell laptop with an LCD screen (1280×1024 pixel resolution) using E-Prime 2.0 software and analyzed using R (v3.5.3) within RStudio (v1.2.1355).

2.3. In-scanner eye-tracking

Eye-tracking data in the fMRI scanner was collected on a SR Research EyeLink 1000+ system in a subsample (n = 10) with demographics representative of the full sample. A larger subsample was unable to be collected as eye-tracking equipment was not available until later in this study. We examined the duration of central fixation within an area <150

pixels radius from center. Fixations were identified by the absence of saccades (velocity threshold = 30°/s) and blink events.

2.4. Neuroimaging acquisition

All data were obtained from a 3 Tesla Siemens scanner at the Yale Magnetic Resonance Research Center in New Haven, CT using a 32 (n = 13) or 64 (n = 20) channel phased array head coil. Prior to acquiring BOLD images, high-resolution T1w and T2w structural images were collected with 0.8 mm isotropic voxels in 224 AC-PC aligned slices, in compliance with the adult Human Connectome Project (HCP) acquisition protocol. T1w images were collected with a magnetization-prepared rapid gradient-echo (MP-RAGE) pulse sequence (TR = 2400 ms, TE = 2.07 ms, flip angle = 8°, field of view = 256×256 mm). T2w images were collected with SPC (SPACE: sampling perfection with application-optimized contrasts using different flip angle evolution (Siemens)) (pulse sequence [TR = 3200 ms, TE = 564 ms, flip angle mode = T2 var, field of view = 256×256 mm]. A pair of reverse phase-encoded spin-echo field maps (anterior to posterior, and posterior to anterior) was also collected to aid distortion correction in preprocessing (voxel size = 2.5 mm isotropic, TR = 7220 ms, TE = 73 ms, flip angle = 90°, field of view = 210×210 mm, bandwidth = 2290 Hz).

All BOLD images were acquired with specifications based on the adult HCP acquisition protocols at the time of collection. 54 interleaved axial slices were collected parallel to the anterior-posterior commissure (AC-PC) with 2.5 mm isotropic voxels using a multi-band accelerated fast gradient-echo, echo-planar sequence (acceleration factor = 6, time repetition (TR) = 700 ms, time echo (TE) = 31.0 ms, flip angle = 55°, field of view = 210×210 mm, matrix = 84×84, bandwidth = 2290 Hz). Each run was 9.33 min with 800 vol. Single-band reference images acquired before each BOLD run aided registration during preprocessing.

2.5. Neuroimaging processing

Structural and functional MRI data were pre-processed using HCP minimal preprocessing pipelines (Glasser et al., 2013) implemented through our multi-modal neuroimaging platform called Quantitative Neuroimaging Environment and Toolbox (Qu|Nex, https://qunex.yale.edu). The open-source HCP pipelines represent the current state-of-the-art in BOLD distortion correction, registration, and maximization of high-resolution signal-to-noise, and have been optimized for our specific acquisition parameters and Yale's High Performance Computing resources (Ji et al., 2019). T1w and T2w images were corrected for bias-field distortions and warped to the standard Montreal Neurological Institute-152 (MNI-152) brain template using the FMRIB Software Library (FSL) linear image registration tool (FLIRT) and non-linear image registration tool (FNIRT) (Jenkinson et al., 2012). Next, FreeSurfer's recon-all pipeline computed brain-wide segmentation of gray and white matter. Cortical surface models were generated for pial and white matter boundaries, and segmentation masks were generated for each subcortical gray matter voxel. A cortical ribbon was defined along with corresponding subcortical voxels, which were combined to generate the Connectivity Informatics Technology Initiative (CIFTI) volume/surface gray-ordinate space for each individual subject. CIFTI format significantly reduces file management for combined surface and volume analyses and establishes a combined cortical surface and subcortical volume coordinate system (Glasser et al., 2013). The cortical

surfaces were registered to the group average HCP atlas using surface-based registration, whereas the subcortical volume component of the image was brought into group atlas alignment via non-linear registration (Glasser et al., 2013).

BOLD data were motion corrected and aligned to the single-band reference images via FLIRT. A liberal brain-mask was applied to exclude signal from non-brain tissue. After initial processing in NIFTI volume space, BOLD data were converted to the CIFTI matrix by sampling from the anatomically-defined gray matter cortical ribbon. Subcortical voxels were isolated using subject-specific FreeSurfer segmentation. The subcortical volume component aligned to the group atlas as part of the NIFTI processing in a single transform step that concatenates all of the transform matrices for each prior processing step (i.e. motion correction, registration, distortion correction) and minimizes interpolation cost. The cortical surface component of the CIFTI file was aligned to the HCP atlas using surface-based nonlinear deformation based on sulcal features. Images were sampled at 2 mm isotropic voxels, consistent with HCP protocols (Glasser et al., 2013). Functional images were smoothed with a 2 mm FWHM Gaussian kernel.

2.6. fMRI analyses

All general linear models were calculated for each subject using inhouse software (Qu|Nex) implemented in Matlab, with 12 motion regressors of no interest, baseline and drift regressors for each run. For assumed response modeling, task regressors for each epoch and condition were included. The hemodynamic response function (HRF) was modeled using an assumed boxcar function convolved with a gamma function (Boynton et al., 1996). Beta coefficients of interest were entered into second-level, random-effects analyses using non-parametric statistics implemented through Permutation Analysis of Linear Models (PALM) software (Winkler et al., 2014). Time courses were reconstructed using a finite impulse response (FIR) model for unassumed HRF modeling in which separate regressors for each of the timepoints of each type of trial were entered into a GLM.

Whole-brain analyses used 5000 permutations, and threshold-free cluster enhancement (TFCE) unless otherwise noted. TFCE approaches cluster correction by calculating a weighted sum of a local cluster signal, thereby avoiding the need to arbitrarily set a cluster threshold for significance (Smith and Nichols, 2009). The first analysis tested for a main effect of sWM across the whole brain (sWM > Motor, across encoding and delay epochs) to ensure that our task design activated canonical sWM regions ($p < 0.05$, whole-brain, family-wise error (FWE-corrected)). We next tested for overlapping regions between sWM neural systems and regions that were impacted by the main effect of cued incentive. For this, a conjunction (logical AND) approach was used to identify regions of overlap between the sWM map and the main effect of cued incentive (each thresholded at $p < 0.05$, FWE-corrected, 5000 permutations, TFCE prior to conjunction). Similar conjunction approaches have been done in prior work on incentivized WM (Pochon et al., 2002). Following this, we tested a 3-way conjunction that involved the aforementioned map of sWM, the aforementioned main effect of cued incentive (Neutral vs. Cued Gain vs. Cued Loss) and an interaction of cued incentive and epoch ((Neutral vs. Cued Gain vs. Cued Loss) x (Encoding vs. Delay)). The latter map was included because neural effects across

various regions of the brain may differ with encoding and delay. While there are behavioral results suggesting that rewards need to be cued prior to, or at, encoding, rather than after encoding, in order to influence WM (Wallis et al., 2015; Brissenden et al., 2021), there is no guarantee that this finding applies throughout the various widespread and diverse regions of the brain. Each map was whole-brain thresholded at $p < 0.05$, FWE-corrected using 5000 permutations and TFCE prior to conjunction. Following this, we tested for overlapping brain regions in which sWM was modulated by incentives that were externally cued, as well as incentives that were internally represented (non-cued). This conjunction tested whether externally cued and internally represented incentives elicited similar effects. To test this we additionally conjuncted a whole-brain corrected map of non-cued incentive (Neutral vs. Non-cued Gain vs. Non-Cued Loss) x epoch (Encoding vs. Delay) to the prior conjunction. For all conjunction analyses, percent signal change was visualized from relative regional peaks in sWM signal in regions that remained after conjunction. To balance the granularity following stringent conjunction with the size of cortical regions, visualized clusters were limited in size between 25 and 600 mm^2 on the cortical surface and 10–250 contiguous voxels in the subcortex. Timecourses were reconstructed using finite impulse response modeling (see earlier).

2.7. Trial-by-Trial fMRI analyses

We used a regression approach to test for regions that showed BOLD signal changes that were associated with improvements in sWM accuracy using a random-effects approach. This allowed us to test for regions in which trial-by-trial incentive-driven sWM improvements were associated with increased BOLD signal during the delay epoch. sWM accuracy for each trial of each subject (except the motor condition) was Z-normalized within-subject and regressed with the associated change in BOLD signal for each trial during the delay epoch at each greyordinate/voxel within the sWM map. This regression was modeled for each subject separately (i.e. within-subject) and resulting regression coefficients were entered into group analyses at each voxel using a one-sample *t*-test ($p < 0.05$, FWE-corrected, 5000 permutations).

ereFor the regions that survived correction, the BOLD signal changes in relation to sWM accuracy were visualized using a rank-order approach. In the first visualization, sWM accuracy for each trial (except motor) was rank-ordered within each subject and then grouped by deciles (10 percent bins) for each subject separately (within-subject). Each decile was entered as a separate regressor into a GLM, and the resulting regressor for each decile was then averaged across subjects for plotting. The unassumed HRF analyses used a finite impulse response approach while the assumed HRF analyses modeled the HRF for each decile during the delay epoch. This provided visualization of the underlying signal changes associated with changes in sWM accuracy. We also illustrated the sWM accuracy associated with BOLD signal changes within conditions, specifically the neutral, cued reward and cued loss conditions within each participant using a similar approach. The spatial working memory accuracy for the neutral, cued reward or cued loss condition were sorted from worst to best for each participant and then stratified into deciles within each condition and each participant (10% bins). The deciles for each condition were entered into a GLM for each participant using an unassumed HRF and assumed HRF approach as

before. Resulting regressors for each decile for each condition (neutral, cued reward or cued loss) were averaged across participants and plotted to visualize the BOLD signal changes associated with sWM accuracy.

Finally, we tested for regions that tracked the trial-by-trial amount and valence of incentive received following sWM performance. The amount of money won or lost in each cued incentive trial was Z-normalized within each condition for each person separately, and regressed for each participant with the change in BOLD signal during feedback at each greyordinate/voxel across the whole brain. Similar to our approach regressing sWM accuracy with BOLD signal changes, this analysis was done using a within-subjects approach. The resulting coefficients for each subject within each condition were entered into group analyses using a one-sample *t*-test ($p < 0.05$, whole-brain FWE-corrected, 5000 permutations, cluster correction ($Z > 2.33$)).

3. Results

3.1. Behavioral effects of incentives on sWM performance

We first tested if gain and loss incentives impacted within-subject sWM performance. Compared to the neutral sWM trials, both gain ($t(32) = 3.92$, $p < 0.001$, $d = 0.68$ (CI: 0.18–1.19)) and loss ($t(32) = 4.21$, $p < 0.001$, $d = 0.73$ (CI: 0.22–1.24)) improved sWM performance across cued and non-cued conditions (main effect of Incentive (neutral, gain, and loss), $F(2,64) = 12.62$, $p < 0.001$) (Fig. 1B). In addition, both cued ($t(32) = 4.94$, $p < 0.001$, $d = 0.82$ (CI:0.44–1.21)) and non-cued ($t(32) = 3.21$, $p < 0.005$, $d = 0.45$ (CI:0.16–0.74)) incentives improved sWM performance compared to the neutral trials (main effect of Cue (neutral, cued and non-cued), ($F(2,64) = 15.7$, $p < 0.001$)) (Fig. 1C). However, this effect was larger for the cued, relative to non-cued, incentive presentations ($t(32) = 2.82$, $p < 0.01$, d = 0.40 (CI:0.11–0.69)). The distribution of responses appeared similar across the incentive conditions (Supplemental Figure 1B). In turn, sWM performance showed correlated effects across conditions (Supplemental Figure 1C). For the neutral block, behavioral performance was similar to that in the neutral ‘catch’ trials, as well as in a block of neutral trials that followed all incentive blocks and were collected as part of a separate experiment, suggesting that presenting neutral trials prior to incentive trials was associated with performance that was similar to when neutral trials were presented after incentive trials (Supplemental Figure 1D). Eye-tracking analyses showed that central fixation did not worsen during motivated sWM conditions (Supplemental Figure 2A, B).

3.2. Brain-wide effects of spatial working memory

We first sought to validate that our task activated canonical neural systems previously shown to be engaged during sWM (Sweeney et al., 1996; Curtis et al., 2004; Geier et al., 2009; Jerde et al., 2012). To test this, we contrasted signal during the neutral sWM condition versus the motor response condition (trials without sWM demands) across both encoding and delay epochs. The resulting map closely matched prior work ($p < 0.05$, family-wise error (FWE) corrected, 5000 permutations) (Fig. 2A, Supplemental Figure 3), and revealed robust fronto-parietal, striatal and cerebellar signal. We illustrated the effects from two cortical areas, the posterior intraparietal sulcus (IPS) (Fig. 2B) and precentral sulcus (PCS)

(Fig. 2C), as prior work has suggested that these two regions are critical for supporting sWM, possibly through organized priority maps of space (Kastner et al., 2007; Jerde et al., 2012; Sprague and Serences, 2013; Mackey et al., 2017) (see Supplemental Figure 3 for an unthresholded map, and Supplemental Figure 4 and Supplemental Table 1 for all areas and coordinates). Collectively, these effects established a baseline, brain-wide sWM map within which the impact of incentives on sWM signal could be examined.

3.3. Effects of cued incentives on neural systems engaged by sWM

We first examined the effects of cued incentives across encoding and delay epochs (i.e., main effect) by testing whether cued incentives modulated sWM signals. We applied a conjunction analysis framework to identify areas across the sWM map (Fig. 3A) that were modulated by cued incentives across the encoding and delay epochs. This conjunction involved: i) the whole-brain map of sWM, included in order to identify the key regions supporting sWM; and ii) the main effect of Cued Incentive (cued gain, cued loss, and neutral), included in order to identify regions impacted by incentives. These maps were statistically orthogonal and independently corrected at the whole-brain level prior to conjunction ($p < 0.05$, FWE-corrected, 5000 permutations).

Regions that remained following this 2-way conjunction, and therefore that demonstrated an effect of cued incentive on sWM regions, included prefrontal and parietal cortices, anterior cingulate cortex, insula cortex, and ventral occipitotemporal cortices (Fig. 3B). As with the brain-wide map of sWM, we illustrate the signal in the IPS and PCS (Kastner et al., 2007; Jerde et al., 2012; Mackey et al., 2017). In the left IPS, elevated BOLD signal was seen during cued gain and loss conditions across encoding and delay epochs, compared to the neutral sWM conditions (Fig. 3C). In the right PCS, BOLD signal was also elevated in the PCS for cued gain and loss conditions across the encoding and delay epochs (Fig. 3E). Two other regions that are commonly implicated in spatial working memory or reward processes, anterior cingulate cortex (ACC) and the superior frontal sulcus (SFS), are also illustrated. In both regions, elevated BOLD signal was seen during cued gain and loss conditions, compared to the neutral condition, across the encoding and delay epochs (Fig. 3D and 3F). See Supplemental Figure 5 and Supplemental Tables 2 and 3 for all areas and coordinates.

To better understand the effects of cued incentives on sWM signals, we next tested whether these effects differentially occurred during the encoding and delay epochs. Building upon our conjunction logic, we applied an additional conjunction analysis to identify areas across the sWM map (Fig. 2A) that were modulated by cued incentives differentially during the encoding or delay epochs. This conjunction involved three statistically orthogonal maps independently corrected at the whole-brain level prior to conjunction ($p < 0.05$, FWE-corrected, 5000 permutations) (Fig. 4A). These maps included the two maps from the prior conjunction (the whole-brain map of sWM and the main effect of Cued Incentive (cued gain, cued loss and neutral)) and a third map, the interaction of Cued Incentive (cued gain, cued loss and neutral) x Epoch (encoding and delay), included in order to identify regions where incentive differentially impacted encoding and delay. Results from this conjunction ensured that identified regions would be engaged by sWM and modulated by cued incentives differentially during encoding and delay epochs.

Overall, the breadth of regions was relatively more restricted, compared to the 2-way conjunction. Regions that remained following this 3-way conjunction, and therefore demonstrated an effect of incentive on sWM signals, included the prefrontal, parietal, cingulate, and ventral occipitotemporal cortices (Fig. 4B). As with the brain-wide map of sWM and the main effect of cued incentives, we continue with illustrating the signal in the IPS and PCS (Kastner et al., 2007; Jerde et al., 2012; Mackey et al., 2017). In the left IPS, separate examination of the epochs demonstrated elevated BOLD signal during the encoding epoch for cued gain trials only; the signal during the cued loss condition appeared similar to that of the neutral sWM trials (Figured 4C, 4D left). During the delay epoch in the IPS there was elevated BOLD signal for both cued gain and loss trials (Fig. 4D right). In the PCS, within both the encoding and delay epoch, BOLD signal was elevated in the PCS for cued gain and loss conditions (Fig. 2F middle and right). In other regions that survived the conjunctions, there appeared to be a heterogeneous impact of cued incentives, as demonstrated by relatively suppressed BOLD signal in anterior prefrontal and parietal areas, and in the cerebellum (Supplemental Figure 6). See Supplemental Figure 6 and Supplemental Tables 4 and 5 for all areas and coordinates. Together, these effects highlighted the distributed neural circuits that are driven by sWM and can be subsequently modulated by incentive cues during sWM epochs.

3.4. Effects of non-cued incentives on neural regions engaged by sWM

Next, we tested if ongoing internal representation of incentives can impact sWM-driven neural signals similarly to the response found from externally cued incentives. We analyzed non-cued incentivized sWM trials, which were visually identical to neutral sWM trials, except for instructions at the start of the block that money could be won (or lost) throughout the block. In other words, no further cues were given at the start of a trial, and no feedback was given, but subjects' performance could continue to be incentivized based on their internal representations of incentive throughout the block. Building upon our prior conjunction logic, we tested whether the previously identified conjunction areas (which were sensitive to cued incentives) were also sensitive to non-cued incentives. To examine this, the prior conjunction was combined with the whole-brain interaction map of Non-Cued Incentive (non-cued gain, non-cued loss, neutral) x Epoch (encoding and delay) ($p < 0.05$, FWE, 5000 permutations, prior to conjunction) (Fig. 5A). This four-way conjunction therefore identified regions that were affected by cued, as well as non-cued, incentives.

The remaining areas in the four-way conjunction were spatially similar, though overall, more restricted, compared to the prior conjunction (Fig. 5B). An illustration of the effects in the IPS showed that this region had elevated BOLD signal during the delay epoch of both non-cued gain and loss conditions, though not during the encoding epoch (Fig. 5C, D). In contrast, the PCS showed consistently elevated BOLD signal for both encoding and delay epochs during non-cued gain and loss trials (Fig. 5E, F), appearing to integrate incentives within both epochs and conditions when incentives were internally represented. As with cued incentives, the effect of non-cued incentives in other regions that survived the conjunction was heterogeneous. Similar to the effect of cued incentives, relative BOLD signal suppression was observed during non-cued incentivized conditions in anterior prefrontal and parietal, and cerebellar areas (Supplemental Figure 7 and Supplemental

Tables 6 and 7). Interestingly, in these regions, as in other regions, the effects of non-cued incentives was also relatively attenuated. Given that the dlPFC, anterior parietal cortex and cerebellum are heterogeneous regions composed of various subdivisions, we overlapped the areas that survived the conjunction with a prior network parcellation schema (Ji et al., 2019) to confirm whether these areas overlapped with traditionally cognitive networks. All three areas with decreased BOLD signal during incentivized sWM were found within the frontoparietal and/or dorsal attention networks (Supplemental Figure 8). In contrast, adjacent areas in the posterior parietal cortex that had elevated BOLD signal during incentivized sWM straddled the visual association network.

3.5. Neural regions associated with trial-by-trial sWM performance

We next sought to understand whether the observed neural changes were associated with trial-by-trial improvements in sWM performance. sWM performance was calculated using the angular distance between the target and response for each trial except motor trials. This yielded a continuous (as opposed to a binary) accuracy measure that could be regressed with BOLD signal during the delay epoch for each trial for each subject, thereby quantifying how much of the BOLD signal during the delay epoch was associated with better sWM performance. We computed this for each voxel across the sWM map identified in Fig. 2A and used a type I voxel-wise error correction. For a select subset of areas, including the posterior IPS and ventral PCS, results revealed an association between increased BOLD signal and better trial-by-trial sWM performance ($p < 0.05$, FWE, 5000 permutations) (Fig. 6A, blue) (Supplemental Table 8). We first visualized this relationship in the IPS across all trial types by rank-ordering the performance of each trial into deciles on a within-subject basis. The first decile referred to the 10% of trials with the worst performance for each subject, and the tenth decile referred to the 10% of trials with the best performance for each subject. A GLM was used to compute the regressors associated with each decile for each subject, and the resulting beta weights for each subject were averaged across subjects and visualized for each decile (Fig. 6B).

This allowed for a direct visualization of the relationship between BOLD signal and sWM performance across all trial types in the IPS, as depicted by the whole-map analysis. We further examined this association between BOLD signal and sWM performance by using the same decile ranking approach to illustrate the increase in BOLD signal within incentive conditions. This illustration revealed a robust association between increased BOLD signal and better sWM performance in each condition (Fig. 6C). Notably, the slopes of the trend lines reflecting the relationship between BOLD signal and sWM performance appeared similar between the neutral, cued gain and cued loss conditions, though overall BOLD signal was greater in incentive conditions, compared to the neutral condition (Fig. 6C).

3.6. Neural regions encoding trial-by-trial valence and performance-driven parametric value of incentive receipt

A key feature of this paradigm involved receiving an incentive amount based on sWM performance. More money was won or avoided in loss for trials with better sWM performance; worse sWM performance resulted in more money lost or less money won. Thresholds for incentives were parameterized and individualized based on how well a person

performed during the neutral sWM condition (see Methods). This allowed us to test the association of trial-by-trial incentive receipt with BOLD signal during the feedback epoch of cued incentive sWM trials. We quantified this relationship by regressing the amount of money won or lost on each cued incentive trial with the BOLD signal during the feedback phase. We computed this effect at the whole-brain level independent of prior analyses because this feedback epoch required no sWM demand; rather this epoch was viewed as incentive receipt that was performance-dependent following a cognitive task (Fig. 7A, $p < 0.05$, FWE, 5000 permutations). Whole-brain corrected effects revealed that larger amounts of money won (gain) was associated with greater BOLD signal across several areas typically implicated in reward processing, including bilateral ventral striatum (VS), putamen, and left ACC/medial PFC (Fig. 7A, B, C) (Supplemental Table 9). Interestingly, larger amounts of averted monetary loss (i.e., less money lost during loss conditions) were also associated with greater BOLD signal across similar reward-related areas, some of which fully overlapped with the areas tracking monetary gain (Fig. 7A, B, C) (Supplemental Table 10). In contrast, increasing amounts of monetary loss was associated with greater signal in areas implicated in disappointment and pain (Vogt et al., 2005; Bromberg-Martin and Hikosaka, 2011; Roy et al., 2014; Fazeli and Buchel, 2018), including bilateral habenula, periaqueductal gray (PAG), and anterior insula (Fig. 7A, B, C) (Supplemental Table 11). Notably, the VS was associated with both monetary gain and averted monetary loss. Therefore, we specifically tested if the VS BOLD signal reflected individual differences in sensitivity to gain receipt and averting loss. There was a significant correlation in the VS BOLD signal demonstrating that participants who were most responsive to the greatest monetary gain were also those who had high VS signal when they most successfully averted monetary loss (left VS effect; $r = 0.59$, $p < 0.001$; right VS, $r = 0.34$, $p = 0.051$). Collectively, these results suggest that the neural circuits involved in incentive receipt following a cognitive task can be distinguished by valence and amount in subcortical and cortical regions.

4. Discussion

Motivational influences on cognition are required for successful goal-directed behaviors. Using an incentivized sWM neuroimaging paradigm based on the original oculomotor delayed response task, we found that monetary gain and loss modulated sWM-related BOLD signal across a distributed set of sWM-evoked areas. Overall, the possibility for monetary gain or loss improved sWM performance, and increased BOLD signal in posterior frontal and parietal regions. Posterior IPS and PCS, areas critical for supporting sWM, specifically had elevated BOLD signal during incentivized sWM that was greater than the BOLD signal changes observed during baseline, neutral sWM. The effect of incentives on sWM-related BOLD signal was heterogeneous, and anterior prefrontal, parietal and cerebellar areas overlapping executive networks displayed relatively decreased BOLD signal. Externally cued incentive presentation and internally represented incentives (non-cued condition) had similar effects on BOLD signal across the brain, suggesting that both types of incentive presentation were capable of eliciting BOLD signal modulation in sWM systems. Linkages between sWM performance and BOLD signal changes were observed in a subset of sWM regions, including in the posterior IPS and PCS, which had greater trial-by-trial BOLD signal changes that were associated with better sWM performance. Incentive receipt was

linked to sWM performance, and the amount of money won or lost was distinguished during feedback in a trial-by-trial manner in distinct neural systems that are known to process pleasure, pain and disappointment. Altogether, our work highlights the complex sensory processes recruited when sWM is motivated, and suggests that BOLD signal changes in the IPS and PCS may be a potential mechanism for motivation-associated improvements in sWM.

4.1. Cued and non-cued incentives improve sWM performance

Sharpened cognition allows an organism to execute actions with greater proficiency than typically mustered (Pessoa and Engelmann, 2010). Overall, we found that the possibility of either monetary gain or loss improved sWM precision, an effect in line with prior work showing incentive-driven effects on cognition (Gilbert and Fiez, 2004; Engelmann and Pessoa, 2007; Locke and Braver, 2008; Longe et al., 2009; Jimura et al., 2010; Klink et al., 2017). Additionally, sWM performance improved when the possibility for incentives was maintained by internal representations as well as cues at the start of each sWM trial. However, behavioral effects were overall stronger for cued incentives, compared to non-cued incentives, likely reflecting the salience of visual stimuli (Krebs et al., 2015), and similar for loss and gain conditions. Eye-tracking analyses in a subset of participants suggested that the improvement in incentivized sWM performance was not due to shifting strategies related to worse central fixation; in fact, under incentivized sWM conditions, participants showed relatively better central fixation, a finding echoed in prior work of humans and monkeys (Leon and Shadlen, 1999; Roesch and Olson, 2005; Kennerley and Wallis, 2009; Cho et al., 2018).

4.2. Incentive engagement of visual and posterior frontoparietal association cortices is associated with better sWM precision

Our work suggests that motivated sWM engages visual association regions of posterior frontoparietal cortices via increased BOLD signal. These regions supported baseline, neutral sWM, as evidenced by the greater BOLD signal during sWM, compared to the motor condition, and also demonstrated even greater BOLD signal when the possibility for monetary reward or loss was presented. Therefore, as with prior studies of motivated working memory, regions that supported cognition also appeared to flexibly integrate incentive-related information (Perlstein et al., 2002; Braver et al., 2009). Our findings additionally suggest that complex sensory processes may be important for supporting cognition under motivated conditions when incentives are externally cued and also internally represented. Prior work has demonstrated that visual association areas are sensitive to incentive information (Rothkirch and Sterzer, 2015), including reward receipt (Weil et al., 2010; Arsenault et al., 2013) and reward cues (Serences, 2008; Stanisor et al., 2013; Cicmil et al., 2015; Zold and Hussain Shuler, 2015). Such sensitivity has been postulated to arise from shifts in attention (Pessoa and Engelmann, 2010; Chelazzi et al., 2013; Stanisor et al., 2013) as well as changes in dopamine release (Arsenault et al., 2013; Takakuwa et al., 2018), which collectively improve encoding and detection of relevant stimuli (Goltstein et al., 2018). Salient physical features of visual stimuli may interact with reward-value associations to enhance encoding by the visual system (Krebs et al., 2015; Hickey and Peelen, 2017; Bachman et al., 2020). Such enhanced encoding may also relate to prior

reward-related associations (Anderson, 2019) and has the possibility for contributing to future decision-making processes (Platt and Glimcher, 1999; Yang and Shadlen, 2007). Similar reward responsiveness has been observed in posterior frontal areas such as the PCS (and surrounding BA 6/8) and frontal eye fields (Amador et al., 2000; Roesch and Olson, 2003; Pastor-Bernier and Cisek, 2011). Taken together, these findings suggest that posterior frontoparietal visual association regions both support baseline sWM and are key for integrating motivational processes with sWM.

Overall, our work is in line with prior neuroimaging studies on motivated working memory with some key differences. In general, prior neuroimaging studies of motivated cognition have demonstrated BOLD signal changes in regions that typically support the baseline cognitive process, usually in prefrontal and parietal cortical regions. Most of these studies, including ours, have used money as an incentive, though it is worth noting that a study by Beck and colleagues demonstrated that the type of incentive may affect which regions support motivated working memory (Beck et al., 2010). In our work, regions that supported working memory were impacted by incentives, and we demonstrated that the effect of incentive within sWM regions was heterogeneous—that is, incentives did not uniformly affect sWM regions through increased BOLD signal. These differential effects likely reflect the heterogeneous nature of the prefrontal cortex, which contains diverse subregions distinguished by cytoarchitecture and connectivity (Barbas and Pandya, 1987; Pandya and Yeterian, 1990; Yeterian and Pandya, 1991; Yeterian et al., 2012). This heterogeneous effect of motivated working memory on prefrontal BOLD signals has previously been seen in other work, with relatively decreased BOLD signals in ventrolateral and ventromedial PFC, and BA10 previously reported (Pochon et al., 2002; Gilbert and Fiez, 2004; Longe et al., 2009). Our results most closely match studies of motivated object or visual WM, both of which typically require visual association cortex during baseline WM, and also when incentive information is integrated (Taylor et al., 2004; Krawczyk et al., 2007; Krawczyk and D'Esposito, 2013). In the case of the study by Taylor and colleagues, which used a delay response visual WM task, elevated BOLD activation was seen in the IPS and superior frontal sulcus, similar to our study (Taylor et al., 2004). Studies of letter n-back working memory and verbal working memory, however, appear to activate more anterior prefrontal regions during reward conditions (Pochon et al., 2002; Gilbert and Fiez, 2004; Longe et al., 2009; Beck et al., 2010; Jimura et al., 2010; Belayachi et al., 2015). These studies have demonstrated elevated BOLD signal during motivated working memory in the dlPFC, as well as other anterior frontal cortical regions. In contrast, our study demonstrated relatively decreased BOLD signal during incentivized sWM in the dlPFC, anterior parietal cortex and cerebellar areas that straddled frontoparietal/dorsal attention networks. This surprising finding may be considered within two broader contexts. The first relates to the type of working memory task used here. We chose to use a spatial working memory task, given the myriad of work using this task in non-human primates that has yielded neuroscientific insights. Spatial working memory tasks elicit delay-related neuronal activity in a variety of regions, including the dlPFC, FEF, visual cortices, and thalamus. In humans, neuroimaging work using sWM has consistently demonstrated the importance of the PCS, the superior frontal sulcus and the posterior IPS in supporting sWM (Courtney et al., 1998; Curtis et al., 2004; Kastner et al., 2007; Jerde et al., 2012; Mackey et al., 2017). While the dlPFC

has been shown to be involved in sWM, and indeed was the original region of interest in classic non-human primate studies and also showed clear involvement in our baseline, neutral sWM trials, lesion studies suggest that its involvement is not necessarily critical for supporting sWM processes in humans (Mackey et al., 2016a, 2016b; Curtis and Sprague, 2021). It is possible that WM tasks requiring maintenance of spatial locations rely more on distributed regions of the visual system to support mnemonic information (Postle, 2006) that can then be integrated with reward signals. In monkeys, work using a rewarded sWM task has demonstrated stronger neuronal firing in posterior frontal regions, including premotor cortex, and FEF, but relatively weaker firing in anterior regions such as dlPFC during rewarded sWM (Roesch and Olson, 2003). Furthermore, neurons in the ventrolateral PFC have been shown to encode reward and sWM more strongly than neurons in the dorsolateral PFC (Kennerley and Wallis, 2009).

The second context of note relates to the task design. In our task, the stimuli signaling incentives and the stimuli for encoded spatial location were simultaneously presented. In the cued condition, signals for gain, loss or neutral conditions were intermixed and pseudorandomly presented but always presented at the spatial location to be encoded. Thus the visual features associated with incentive, here color, may have had enhanced salience that led to engagement of the visual system, with concomitant suppression of executive systems (Krebs et al., 2015). In the dlPFC, the BOLD signal activation seen during baseline sWM and the relative BOLD signal suppression seen during incentivized conditions may also be reflective of the dual modes of ‘proactive’ and ‘reactive’ engagement of cognitive systems, as described by the dual-mechanisms theory of cognitive control (Aron, 2011; Braver, 2012). ‘Reactive’ engagement, which is described as cognitive engagement that occurs in response to salient or interfering events, may have been particularly relevant when incentive cues were intermittently presented and presented at the spatial location to be encoded. This is in contrast with ‘proactive’ engagement, which requires ongoing maintenance and updating of goal-directed or rule-based information. While studies in monkeys have shown increased neuronal firing in the dlPFC during rewarded sWM trials, notably, this has occurred when rewards were presented after a group of sWM trials and in trials that were closer in time to the rewarded trial (Ichihara-Takeda and Funahashi, 2008). While this could reflect integration of reward and working memory, it is also possible that this observation could reflect ongoing maintenance of reward schedules and specific preparation for an upcoming rewarded trial. In other monkey studies, it has been observed that dlPFC neuronal firing begins after the spatial location is cued when the incentive cue and spatial cue are dissociated (Leon and Shadlen, 1999). Therefore, it is possible that the co-presentation of incentive information and spatial location in our task may have limited the ability of participants to prepare a cognitive response.

Finally, a subset of regions involved in visual processing, including the posterior IPS, PCS, MT and other regions appeared to encode trial-by-trial improvements in sWM precision. Higher-order cortical visual areas have been proposed to prioritize spatial awareness based on behavioral relevance (Sprague et al., 2018), and internally-driven attentional demands, such as those that would be required in sWM tasks (Kastner et al., 2007; Silver and Kastner, 2009; Jerde et al., 2012; Mackey et al., 2017). In these regions topographic priority maps have been demonstrated that support spatial representations during working

memory (Sprague and Serences, 2013). Though further work is needed, it is possible that shifts in internal representations of spatial priorities may also be a mechanism for incentive-driven sWM improvements, with posterior prefrontal regions possibly shaping sWM representations in posterior parietal regions to improve sWM accuracy (Merrikhi et al., 2017). Overall, the IPS and PCS appeared to be regions that linked changes in sWM performance with changes in neural signals.

4.3. Receipt of feedback regarding incentive valence and amount of monetary outcome is encoded across distinct areas

Incentives are maximally salient when received after an action, compared to when passively received in the absence of an action (Zink et al., 2004). In our paradigm design, increasing amounts of money were gained, or avoided in loss, on trials with better sWM performance, linking the salience of the action (i.e. better sWM performance) with the incentive-related outcome (i.e. receipt of money). While gain and loss appeared to impact sWM neural circuits in a similar way during encoding and delay periods, we observed differences during the trial-by-trial receipt of incentive feedback at the end of each trial. Gaining more money during the feedback epoch was associated with greater trial-by-trial BOLD signal across regions with well-established reward-related responses, including bilateral ventral striatum (VS) and medial PFC (Knutson et al., 2001; Jessup and O'Doherty, 2014). Greater amounts of money avoided in loss were associated with trial-by-trial increases in BOLD signal in the ventral striatum, putamen and parietal cortex. Interestingly, receiving increasing amounts of money and avoiding more monetary loss led to overlapping BOLD signal changes in the ventral striatum/putamen, and the precuneus. In the ventral striatum, people who were most sensitive to gain receipt appeared to also be the most sensitive to avoiding loss. Finally, greater amounts of monetary loss led to higher trial-by-trial BOLD signals in regions typically linked to pain or disappointment, including the habenula, anterior insula, PAG, and ACC (Vogt, 2005; Bromberg-Martin and Hikosaka, 2011; Roy et al., 2014; Fazeli and Buchel, 2018). Thus, while the effects of loss and gain were similar during sWM encoding and delay epochs, they appeared distinguished during the feedback phase across distinct brain systems (Reynolds and Berridge, 2002; Tye, 2018; Berridge, 2019), suggesting that brain systems differentially track incentive valence following a cognitive process.

4.4. Limitations and future directions

Of note, all conjunction analyses focused on how incentives specifically impacted areas engaged during sWM. Therefore, this study did not test whether incentives modulated brain regions irrespective of sWM engagement. Future experiments may also explicitly dissociate the incentive cue and context from the encoding phase of the sWM task to test for the interaction between incentives and spatial location encoding, and whether more preparatory processes can be engaged. Eye-tracking data was collected only in a subset of the sample due to practical constraints, as equipment was not available until later in the study. Nevertheless, our findings were similar to studies in non-human primates and our previously published human study with a larger sample size (Leon and Shadlen, 1999; Roesch and Olson, 2003; Kennerley and Wallis, 2009; Cho et al., 2018). Finally, this incentive-driven sWM paradigm offers a possible platform to develop clinically-relevant

markers of both affect and cognitive computational disruptions across populations of patients with psychiatric illnesses.

5. Conclusions

Here, we provide evidence that posterior frontoparietal regions involved in visual association processes integrate motivation with sWM neural signals. Using fMRI and our incentivized sWM paradigm we found that cued and non-cued incentives improved sWM accuracy, and enhanced BOLD signals within the posterior IPS and PCS, visual association regions that also support baseline sWM processes. Furthermore, the trial-by-trial improvements in sWM were associated with BOLD signal increases in the IPS and PCS, suggesting that these regions may be important for linking sWM accuracy with neural signal changes. In contrast, regions within the anterior prefrontal and parietal cortices and cerebellum had relative decreases in BOLD signal during incentivized sWM conditions, compared to the baseline, neutral sWM condition. Better sWM performance was associated with more money won or avoided in loss, and trial-by-trial changes in the amount of money won, lost or avoided in loss was associated with BOLD signal changes in regions that could be distinguished as processing positively or negatively valenced stimuli. Taken together this work provides evidence that the posterior IPS and PCS may be key regions that link neural changes with motivated sWM and highlights the complex sensory processes that may be recruited when sWM is motivated.

Supplementary Material

Refer to Web version on PubMed Central for supplementary material.

Acknowledgements

The authors thank Bill Martin, PhD, for helpful conversations around task conceptualization.

Funding Sources

This work was supported by the NARSAD Independent Investigator Award, 1DP5-OD012109 (PI: Anticevic, A.), the NARSAD Young Investigator Award (PI: Cho, Y.), the Thomas P. Detre Fellowship in Neuroscience at Yale University (PI: Cho, Y.), K23 MH121778 (PI: Cho, Y.), T32 MH019961 (Cho, Y.; PI: Robert T. Malison), T32 MH018268 (Cho, Y.; PI: Michael J. Crowley), and J3–9264 (Slovenian Research Agency (ARRS); PI: Repovs, G.). This work was funded in part by the State of Connecticut, Department of Mental Health and Addiction Services, but this publication does not express the views of the Department of Mental Health and Addiction Services or the State of Connecticut. The views and opinions expressed are those of the authors.

Data availability statement

For Cho et al. Reward and Loss Incentives Improve Spatial Working Memory by Shaping Trial-by-Trial Posterior Frontoparietal Signals Neuroimaging data will be uploaded for public sharing on BALSA, https://balsa.wustl.edu.

References

Aarts E, van Holstein M, Cools R, 2011. Striatal Dopamine and the Interface between Motivation and Cognition. Front. Psychol. 2, 163. [PubMed: 21808629]

Aarts E, van Holstein M, Hoogman M, Onnink M, Kan C, Franke B, Buitelaar J, Cools R, 2015. Reward modulation of cognitive function in adult attention-deficit/hyperactivity disorder: a pilot study on the role of striatal dopamine. Behav. Pharmacol. 26, 227–240. [PubMed: 25485641]

Amador N, Schlag-Rey M, Schlag J, 2000. Reward-predicting and reward-detecting neuronal activity in the primate supplementary eye field. J. Neurophysiol. 84, 2166–2170. [PubMed: 11024104]

Anderson BA, 2019. Neurobiology of value-driven attention. Curr. Opin. Psychol. 29, 27–33. [PubMed: 30472540]

Anticevic A, Schleifer C, Cho YT, 2015. Emotional and cognitive dysregulation in schizophrenia and depression: understanding common and distinct behavioral and neural mechanisms. Dialogues Clin. Neurosci. 17, 421–434. [PubMed: 26869843]

Aron AR, 2011. From reactive to proactive and selective control: developing a richer model for stopping inappropriate responses. Biol. Psychiatry 69, e55–e68. [PubMed: 20932513]

Arsenault JT, Nelissen K, Jarraya B, Vanduffel W, 2013. Dopaminergic reward signals selectively decrease fMRI activity in primate visual cortex. Neuron 77, 1174–1186. [PubMed: 23522051]

Bachman MD, Wang L, Gamble ML, Woldorff MG, 2020. Physical Salience and Value-Driven Salience Operate through Different Neural Mechanisms to Enhance Attentional Selection. J. Neurosci. 40, 5455–5464. [PubMed: 32471878]

Barash S, Bracewell RM, Fogassi L, Gnadt JW, Andersen RA, 1991. Saccade-related activity in the lateral intraparietal area. II. Spatial properties. J. Neurophysiol. 66, 1109–1124. [PubMed: 1753277]

Barbas H, Mesulam MM, 1981. Organization of afferent input to subdivisions of area 8 in the rhesus monkey. J. Comp. Neurol. 200, 407–431. [PubMed: 7276245]

Barbas H, Pandya DN, 1987. Architecture and frontal cortical connections of the premotor cortex (area 6) in the rhesus monkey. J. Comp. Neurol. 256, 211–228. [PubMed: 3558879]

Beck SM, Locke HS, Savine AC, Jimura K, Braver TS, 2010. Primary and secondary rewards differentially modulate neural activity dynamics during working memory. PLoS ONE 5, e9251. [PubMed: 20169080]

Belayachi S, Majerus S, Gendolla G, Salmon E, Peters F, Van der Linden M, 2015. Are the carrot and the stick the two sides of same coin? A neural examination of approach/avoidance motivation during cognitive performance. Behav. Brain Res. 293, 217–226. [PubMed: 26213335]

Berridge KC, 2009. Wanting and Liking: observations from the Neuroscience and Psychology Laboratory. Inquiry (Oslo) 52, 378. [PubMed: 20161627]

Berridge KC, 2012. From prediction error to incentive salience: mesolimbic computation of reward motivation. Eur. J. Neurosci. 35, 1124–1143. [PubMed: 22487042]

Berridge KC, 2019. Affective valence in the brain: modules or modes? Nat. Rev. Neurosci. 20, 225–234. [PubMed: 30718826]

Berridge KC, Robinson TE, Aldridge JW, 2009. Dissecting components of reward: ‘liking’, ‘wanting’, and learning. Curr. Opin. Pharmacol. 9, 65–73. [PubMed: 19162544]

Bisley JW, Zaksas D, Droll JA, Pasternak T, 2004. Activity of neurons in cortical area MT during a memory for motion task. J. Neurophysiol. 91, 286–300. [PubMed: 14523065]

Botvinick M, Braver T, 2015. Motivation and cognitive control: from behavior to neural mechanism. Annu. Rev. Psychol. 66, 83–113. [PubMed: 25251491]

Boynton GM, Engel SA, Glover GH, Heeger DJ, 1996. Linear systems analysis of functional magnetic resonance imaging in human V1. J. Neurosci. 16, 4207–4221. [PubMed: 8753882]

Braver TS, 2012. The variable nature of cognitive control: a dual mechanisms framework. Trends Cogn. Sci. 16, 106–113. [PubMed: 22245618]

Braver TS, Paxton JL, Locke HS, Barch DM, 2009. Flexible neural mechanisms of cognitive control within human prefrontal cortex. Proc. Natl. Acad. Sci. U. S. A. 106, 7351–7356. [PubMed: 19380750]

Braver TS, et al. , 2014. Mechanisms of motivation-cognition interaction: challenges and opportunities. Cogn. Affect. Behav. Neurosci. 14, 443–472. [PubMed: 24920442]

Brissenden JA, Adkins TJ, Hsu YT, Lee TG, 2021. Reward Influences the Allocation But Not the Availability of Resources in Visual Working Memory. BioRxiv.

Bromberg-Martin ES, Hikosaka O, 2011. Lateral habenula neurons signal errors in the prediction of reward information. Nat. Neurosci. 14, 1209–1216. [PubMed: 21857659]

Cavada C, Gol dman-Rakic PS, 1991. Topographic segregation of corticostriatal projections from posterior parietal subdivisions in the macaque monkey. Neuroscience 42, 683–696. [PubMed: 1720224]

Chafee MV, Goldman-Rakic PS, 1998. Matching patterns of activity in primate prefrontal area 8a and parietal area 7ip neurons during a spatial working memory task. J. Neurophysiol. 79, 2919–2940. [PubMed: 9636098]

Chelazzi L, Perlato A, Santandrea E, Della Libera C, 2013. Rewards teach visual selective attention. Vision Res. 85, 58–72. [PubMed: 23262054]

Cho YT, Lam NH, Starc M, Santamauro N, Savic A, Diehl CK, Schleifer CH, Moujaes F, Srihari VH, Repovs G, Murray JD, Anticevic A, 2018. Effects of reward on spatial working memory in schizophrenia. J. Abnorm. Psychol. 127, 695–709. [PubMed: 30335439]

Cicmil N, Cumming BG, Parker AJ, Krug K, 2015. Reward modulates the effect of visual cortical microstimulation on perceptual decisions. Elife 4, e07832. [PubMed: 26402458]

Collins AG, Brown JK, Gold JM, Waltz JA, Frank MJ, 2014. Working memory contributions to reinforcement learning impairments in schizophrenia. J. Neurosci. 34, 13747–13756. [PubMed: 25297101]

Collins AGE, Albrecht MA, Waltz JA, Gold JM, Frank MJ, 2017. Interactions Among Working Memory, Reinforcement Learning, and Effort in Value-Based Choice: a New Paradigm and Selective Deficits in Schizophrenia. Biol. Psychiatry 82, 431–439. [PubMed: 28651789]

Compte A, Brunel N, Goldman-Rakic PS, Wang XJ, 2000. Synaptic mechanisms and network dynamics underlying spatial working memory in a cortical network model. Cereb. Cortex 10, 910–923. [PubMed: 10982751]

Constantinidis C, Steinmetz MA, 1996. Neuronal activity in posterior parietal area 7a during the delay periods of a spatial memory task. J. Neurophysiol. 76, 13521355.

Courtney SM, Peti L, Maisog JM, Ungerleider LG, Haxby JV, 1998. An area specialized for spatial working memory in human frontal cortex. Science 279, 13471351.

Curtis CE, Sprague TC, 2021. Persistent Activity During Working Memory From Front to Back. Front. Neural Circuits 15, 66060.

Curtis CE, Rao VY, D'Esposit M, 2004. Maintenance of spatial and motor codes during oculomotor delayed response tasks. J. Neurosci. 24, 39443952.

Dixon ML, Christof K, 2012. The decision to engage cognitive control is driven by expected reward-value: neural and behavioral evidence. PLoS ONE 7, e1637.

Durstewit D, Seamans JK, Sejnowski TJ, 2000. Dopamine-mediated stabilization of delay-period activity in a network model of prefrontal cortex. J. Neurophysiol. 83, 17331750.

Engelmann JB, Pesso L, 2007. Motivation sharpens exogenous spatial attention Emotion 7, 66–674.

Fazeli S, Buchel C, 2018. Pain-Related Expectation and Prediction Error Signals in the Anterior Insula Are Not Related to Aversiveness. J. Neurosci. 38, 6461–6474. [PubMed: 29934355]

Funahashi S, Bruce CJ, Goldman-Rakic PS, 1989. Mnemonic coding of visual space in the monkey's dorsolateral prefrontal cortex. J. Neurophysiol. 61, 331–349. [PubMed: 2918358]

Fuster JM, 1973. Unit activity in prefrontal cortex during delayed-response performance: neuronal correlates of transient memory. J. Neurophysiol. 36, 61–78. [PubMed: 4196203]

Geier CF, Garver K, Terwilliger R, Luna B, 2009. Development of working memory maintenance. J. Neurophysiol. 101, 84–99. [PubMed: 18971297]

Geier CF, Terwilliger R, Teslovich T, Velanova K, Luna B, 2010. Immaturities in reward processing and its influence on inhibitory control in adolescence. Cereb. Cortex 20, 1613–1629. [PubMed: 19875675]

Gilbert AM, Fiez JA, 2004. Integrating rewards and cognition in the frontal cortex. Cogn. Affect. Behav. Neurosci. 4, 540–552. [PubMed: 15849896]

Glasser MF, Sotiropoulos SN, Wilson JA, Coalson TS, Fischl B, Andersson JL, Xu J, Jbabdi S, Webster M, Polimeni JR, Van Essen DC, Jenkinson M, Consortium WU-MH, 2013. The minimal

preprocessing pipelines for the Human Connectome Project. Neuroimage 80, 105–124. [PubMed: 23668970]

Goltstein PM, Meijer GT, Pennartz CM, 2018. Conditioning sharpens the spatial representation of rewarded stimuli in mouse primary visual cortex. Elife 7.

Gong M, Li S, 2014. Learned reward association improves visual working memory. J. Exp. Psychol. Hum. Percept. Perform. 40, 841–856. [PubMed: 24392741]

Grahek I, Shenhav A, Musslick S, Krebs RM, Koster EHW, 2019. Motivation and cognitive control in depression. Neurosci. Biobehav. Rev. 102, 371–381. [PubMed: 31047891]

Hickey C, Peelen MV, 2017. Reward Selectively Modulates the Lingering Neural Representation of Recently Attended Objects in Natural Scenes. J. Neurosci. 37, 7297–7304. [PubMed: 28630254]

Hikosaka O, Wurtz RH, 1983. Visual and oculomotor functions of monkey substantia nigra pars reticulata. III. Memory-contingent visual and saccade responses. J. Neurophysiol. 49, 1268–1284. [PubMed: 6864250]

Honig M, Ma WJ, Fougnie D, 2020. Humans incorporate trial-to-trial working memory uncertainty into rewarded decisions. Proc. Natl. Acad. Sci. U. S. A. 117, 8391–8397. [PubMed: 32229572]

Ichihara-Takeda S, Funahashi S, 2008. Activity of primate orbitofrontal and dorsolateral prefrontal neurons: effect of reward schedule on task-related activity. J. Cogn. Neurosci. 20, 563–579. [PubMed: 18052781]

Infanti E, Hickey C, Turatto M, 2015. Reward associations impact both iconic and visual working memory. Vision Res. 107, 22–29. [PubMed: 25481632]

Jenkinson M, Beckmann CF, Behrens TE, Woolrich MW, Smith SM, 2012. Fsl. Neuroimage 62, 782–790. [PubMed: 21979382]

Jerde TA, Merriam EP, Riggall AC, Hedges JH, Curtis CE, 2012. Prioritized maps of space in human frontoparietal cortex. J. Neurosci. 32, 17382–17390. [PubMed: 23197729]

Jessup RK, O'Doherty JP, 2014. Distinguishing informational from value-related encoding of rewarding and punishing outcomes in the human brain. Eur. J. Neurosci. 39, 2014–2026. [PubMed: 24863104]

Ji JL, Spronk M, Kulkarni K, Repovs G, Anticevic A, Cole MW, 2019. Mapping the human brain's cortical-subcortical functional network organization. Neuroimage 185, 35–57. [PubMed: 30291974]

Jimura K, Braver TS, 2010. Age-related shifts in brain activity dynamics during task switching. Cereb. Cortex 20, 1420–1431. [PubMed: 19805420]

Jimura K, Locke HS, Braver TS, 2010. Prefrontal cortex mediation of cognitive enhancement in rewarding motivational contexts. Proc. Natl. Acad. Sci. U. S. A. 107, 8871–8876. [PubMed: 20421489]

Kastner S, DeSimone K, Konen CS, Szczepanski SM, Weiner KS, Schneider KA, 2007. Topographic maps in human frontal cortex revealed in memory-guided saccade and spatial working-memory tasks. J. Neurophysiol. 97, 3494–3507. [PubMed: 17360822]

Kennerley SW, Wallis JD, 2009. Reward-dependent modulation of working memory in lateral prefrontal cortex. J. Neurosci. 29, 3259–3270. [PubMed: 19279263]

Kim H, Shimojo S, O'Doherty JP, 2006. Is avoiding an aversive outcome rewarding? Neural substrates of avoidance learning in the human brain. PLoS Biol. 4, e233. [PubMed: 16802856]

Klink PC, Jeurissen D, Theeuwes J, Denys D, Roelfsema PR, 2017. Working memory accuracy for multiple targets is driven by reward expectation and stimulus contrast with different time-courses. Sci. Rep. 7, 9082. [PubMed: 28831072]

Klyszejko Z, Rahmati M, Curtis CE, 2014. Attentional priority determines working memory precision. Vision Res. 105, 70–76. [PubMed: 25240420]

Knutson B, Adams CM, Fong GW, Hommer D, 2001. Anticipation of increasing monetary reward selectively recruits nucleus accumbens. J. Neurosci. 21, RC159. [PubMed: 11459880]

Krawczyk DC, D'Esposito M, 2013. Modulation of working memory function by motivation through loss-aversion. Hum. Brain Mapp. 34, 762–774. [PubMed: 22113962]

Krawczyk DC, Gazzaley A, D'Esposito M, 2007. Reward modulation of prefrontal and visual association cortex during an incentive working memory task. Brain Res. 1141, 168–177. [PubMed: 17320835]

Krebs RM, Boehler CN, Woldorff MG, 2010. The influence of reward associati onson conflict processing in the Stroop task. Cognition 117, 341–347. [PubMed: 20864094]

Krebs RM, Boehler CN, Egner T, Woldorff MG, 2011. The neural underpinnings of how reward associations can both guide and misguide attention. J. Neurosci. 31, 9752–9759. [PubMed: 21715640]

Krebs RM, Hopf J-M, Boehler CN, 2015. Within-Trial Effects of Stimulus-Reward Associations. In: Braver T (Ed.), Motivation and Cognitive Control. Routledge, pp. 65–82.

Lawrence SJD, van Mourik T, Kok P, Koopmans PJ, Norris DG, de Lange FP, 2018. Laminar Organization of Working Memory Signals in Human Visual Cortex. Curr. Biol. 28, 3435–3440 e3434. [PubMed: 30344121]

Leon MI, Shadlen MN, 1999. Effect of expected reward magnitude on the response of neurons in the dorsolateral prefrontal cortex of the macaque. Neuron 24, 415–425. [PubMed: 10571234]

Locke HS, Braver TS, 2008. Motivational influences on cognitive control: behavior, brain activation, and individual differences. Cogn. Affect. Behav. Neurosci. 8, 99–112. [PubMed: 18405050]

Longe O, Senior C, Rippon G, 2009. The lateral and ventromedial prefrontal cortex work as a dynamic integrated system: evidence from FMRI connectivity analysis. J. Cogn. Neurosci. 21, 141–154. [PubMed: 18476765]

Lundqvist M, Rose J, Herman P, Brincat SL, Buschman TJ, Miller EK, 2016. Gamma and Beta Bursts Underlie Working Memory. Neuron 90, 152–164. [PubMed: 26996084]

Mackey WE, Winawer J, Curtis CE, 2017. Visual field map clusters in human frontoparietal cortex. Elife 6.

Mackey WE, Devinsky O, Doyle WK, Golfinos JG, Curtis CE, 2016a. Human parietal cortex lesions impact the precision of spatial working memory. J. Neurophysiol. 116, 1049–1054. [PubMed: 27306678]

Mackey WE, Devinsky O, Doyle WK, Meager MR, Curtis CE, 2016b. Human Dorsolateral Prefrontal Cortex Is Not Necessary for Spatial Working Memory. J. Neurosci. 36, 2847–2856. [PubMed: 26961941]

Manga A, Vakli P, Vidnyanszky Z, 2020. The influence of anticipated monetary incentives on visual working memory performance in healthy younger and older adults. Sci. Rep. 10, 8817. [PubMed: 32483177]

McCarthy G, Puce A, Constable RT, Krystal JH, Gore JC, Goldman-Rakic P, 1996. Activation of human prefrontal cortex during spatial and nonspatial working memory tasks measured by functional MRI. Cereb. Cortex 6, 600–611. [PubMed: 8670685]

McCarthy G, Blamire AM, Puce A, Nobre AC, Bloch G, Hyder F, Goldman-Rakic P, Shulman RG, 1994. Functional magnetic resonance imaging of human prefrontal cortex activation during a spatial working memory task. Proc. Natl. Acad. Sci. U. S. A. 91, 8690–8694. [PubMed: 8078943]

Merrikhi Y, Clark K, Albarran E, Parsa M, Zirnsak M, Moore T, Noudoost B, 2017. Spatial working memory alters the efficacy of input to visual cortex. Nat. Commun. 8, 15041. [PubMed: 28447609]

Miller EK, Erickson CA, Desimone R, 1996. Neural mechanisms of visual working memory in prefrontal cortex of the macaque. J. Neurosci. 16, 5154–5167. [PubMed: 8756444]

Morey CC, Cowan N, Morey RD, Rouder JN, 2011. Flexible attention allocation to visual and auditory working memory tasks: manipulating reward induces a trade-off. Atten. Percept. Psycho 73, 458–472.

Murray JD, Anticevic A, Gancsos M, Ichinose M, Corlett PR, Krystal JH, Wang XJ, 2012. Linking Microcircuit Dysfunction to Cognitive Impairment: effects of Disinhibition Associated with Schizophrenia in a Cortical Working Memory Model. Cereb. Cortex.

Pandya DN, Yeterian EH, 1990. Prefrontal cortex in relation to other cortical areas in rhesus monkey: architecture and connections. Prog. Brain Res. 85, 63–94. [PubMed: 2094916]

Park SH, Rogers LL, Johnson MR, Vickery TJ, 2021. Reward impacts visual statistical learning. Cogn. Affect. Behav. Neurosci. 21, 1176–1195. [PubMed: 34089142]

Pasternak T, Greenlee MW, 2005. Working memory in primate sensory systems. Nat. Rev. Neurosci. 6, 97–107. [PubMed: 15654324]

Pastor-Bernier A, Cisek P, 2011. Neural correlates of biased competition in premotor cortex. J. Neurosci. 31, 7083–7088. [PubMed: 21562270]

Perlstein WM, Elbert T, Stenger VA, 2002. Dissociation in human prefrontal cortex of affective influences on working memory-related activity. Proc. Natl. Acad. Sci. U. S. A. 99, 1736–1741. [PubMed: 11818573]

Pessoa L, 2017. Cognitive-motivational interactions: beyond boxes-and-arrows models of the mind-brain. Motiv. Sci. 3, 287–303. [PubMed: 29399604]

Pessoa L, Engelmann JB, 2010. Embedding reward signals into perception and cognition. Front. Neurosci. 4.

Petrides M, 2000. Dissociable roles of mid-dorsolateral prefrontal and anterior inferotemporal cortex in visual working memory. J. Neurosci. 20, 7496–7503. [PubMed: 11007909]

Petrides M, Pandya DN, 1999. Dorsolateral prefrontal cortex: comparative cytoarchitectonic analysis in the human and the macaque brain and corticocortical connection patterns. Eur. J. Neurosci. 11, 1011–1036. [PubMed: 10103094]

Platt ML, Glimcher PW, 1999. Neural correlates of decision variables in parietal cortex. Nature 400, 233–238. [PubMed: 10421364]

Pochon JB, Levy R, Fossati P, Lehericy S, Poline JB, Pillon B, Le Bihan D, Dubois B, 2002. The neural system that bridges reward and cognition in humans: an fMRI study. Proc. Natl. Acad. Sci. U. S. A. 99, 5669–5674. [PubMed: 11960021]

Postle BR, 2006. Working memory as an emergent property of the mind and brain. Neuroscience 139, 23–38. [PubMed: 16324795]

Rahmati M, Saber GT, Curtis CE, 2018. Population Dynamics of Early Visual Cortex during Working Memory. J. Cogn. Neurosci. 30, 219–233. [PubMed: 28984524]

Reynolds SM, Berridge KC, 2002. Positive and negative motivation in nucleus accumbens shell: bivalent rostrocaudal gradients for GABA-elicited eating, taste “liking”/“disliking” reactions, place preference/avoidance, and fear. J. Neurosci. 22, 7308–7320. [PubMed: 12177226]

Roesch MR, Olson CR, 2003. Impact of expected reward on neuronal activity in prefrontal cortex, frontal and supplementary eye fields and premotor cortex. J. Neurophysiol. 90, 1766–1789. [PubMed: 12801905]

Roesch MR, Olson CR, 2005. Neuronal activity dependent on anticipated and elapsed delay in macaque prefrontal cortex, frontal and supplementary eye fields, and premotor cortex. J. Neurophysiol. 94, 1469–1497. [PubMed: 15817652]

First Edition Rothkirch M, Sterzer P, 2015. The Role of Motivation in Visual Information Processing. In: Braver T, (Ed.), Motivation and Cognitive Control. Routledge, pp. 23–49 First Edition.

Roy M, Shohamy D, Daw N, Jepma M, Wimmer GE, Wager TD, 2014. Representation of aversive prediction errors in the human periaqueductal gray. Nat. Neurosci. 17, 1607–1612. [PubMed: 25282614]

Sandry J, Ricker TJ, 2020. Prioritization within visual working memory reflects a flexible focus of attention. Atten. Percept. Psycho. 82, 2985–3004.

Schultz W, 2016. Dopamine reward prediction-error signalling: a two-component response. Nat. Rev. Neurosci. 17, 183–195. [PubMed: 26865020]

Serences JT, 2008. Value-based modulations in human visual cortex. Neuron 60, 1169–1181. [PubMed: 19109919]

Silver MA, Kastner S, 2009. Topographic maps in human frontal and parietal cortex. Trends Cogn. Sci. 13, 488–495. [PubMed: 19758835]

Small DM, Gitelman D, Simmons K, Bloise SM, Parrish T, Mesulam MM, 2005. Monetary incentives enhance processing in brain regions mediating top-down control of attention. Cereb. Cortex 15, 1855–1865. [PubMed: 15746002]

Smith SM, Nichols TE, 2009. Threshold-free cluster enhancement: addressing problems of smoothing, threshold dependence and localisation in cluster inference. Neuroimage 44, 83–98. [PubMed: 18501637]

Sprague TC, Serences JT, 2013. Attention modulates spatial priority maps in the human occipital, parietal and frontal cortices. Nat. Neurosci. 16, 1879–1887. [PubMed: 24212672]

Sprague TC, Itthipuripat S, Vo VA, Serences JT, 2018. Dissociable signatures of visual salience and behavioral relevance across attentional priority maps in human cortex. J. Neurophysiol. 119, 2153–2165. [PubMed: 29488841]

Stanisor L, van der Togt C, Pennartz CM, Roelfsema PR, 2013. A unified selection signal for attention and reward in primary visual cortex. Proc. Natl. Acad. Sci. U. S. A. 110, 9136–9141. [PubMed: 23676276]

Steenrod SC, Phillips MH, Goldberg ME, 2013. The lateral intraparietal area codes the location of saccade targets and not the dimension of the saccades that will be made to acquire them. J. Neurophysiol. 109, 2596–2605. [PubMed: 23468388]

Sweeney JA, Mintun MA, Kwee S, Wiseman MB, Brown DL, Rosenberg DR, Carl JR, 1996. Positron emission tomography study of voluntary saccadic eye movements and spatial working memory. J. Neurophysiol. 75, 454–468. [PubMed: 8822570]

Takakuwa N, Redgrave P, Isa T, 2018. Cortical visual processing evokes short-latency reward-predicting cue responses in primate midbrain dopamine neurons. Sci. Rep.8, 14984. [PubMed: 30297792]

Taylor SF, Welsh RC, Wager TD, Phan KL, Fitzgerald KD, Gehring WJ, 2004. A functional neuroimaging study of motivation and executive function. Neuroimage 21, 1045–1054. [PubMed: 15006672]

Thurm F, Zink N, Li SC, 2018. Comparing Effects of Reward Anticipation on Working Memory in Younger and Older Adults. Front. Psychol. 9, 2318. [PubMed: 30546333]

Tye KM, 2018. Neural Circuit Motifs in Valence Processing. Neuron 100, 436–452. [PubMed: 30359607]

van den Berg R, Ma WJ, 2018. A resource-rational theory of set size effects in human visual working memory. Elife 7.

Vijayraghavan S, Wang M, Birnbaum SG, Williams GV, Arnsten AF, 2007. Inverted-U dopamine D1 receptor actions on prefrontal neurons engaged in working memory. Nat. Neurosci. 10, 376–384. [PubMed: 17277774]

Vogt BA, 2005. Pain and emotion interactions in subregions of the cingulate gyrus. Nat. Rev. Neurosci. 6, 533–544. [PubMed: 15995724]

Vogt BA, Vogt L, Farber NB, Bush G, 2005. Architecture and neurocytology of monkey cingulate gyrus. J. Comp. Neurol. 485, 218–239. [PubMed: 15791645]

Wallis G, Stokes MG, Arnold C, Nobre AC, 2015. Reward boosts working memory encoding over a brief temporal window. Vis. Cogn. 23, 291–312.

Weil RS, Furl N, Ruff CC, Symmonds M, Flandin G, Dolan RJ, Driver J, Rees G, 2010. Rewarding feedback after correct visual discriminations has both general and specific influences on visual cortex. J. Neurophysiol. 104, 1746–1757. [PubMed: 20660419]

Wimmer K, Nykamp DQ, Constantinidis C, Compte A, 2014. Bump attractor dynamics in prefrontal cortex explains behavioral precision in spatial working memory. Nat. Neurosci. 17, 431–439. [PubMed: 24487232]

Winkler AM, Ridgway GR, Webster MA, Smith SM, Nichols TE, 2014. Permutation inference for the general linear model. Neuroimage 92, 381–397. [PubMed: 24530839]

Woloszyn L, Sheinberg DL, 2009. Neural dynamics in inferior temporal cortex during a visual working memory task. J. Neurosci. 29, 5494–5507. [PubMed: 19403817]

Yang T, Shadlen MN, 2007. Probabilistic reasoning by neurons. Nature 447, 1075–1080. [PubMed: 17546027]

Yeterian EH, Pandya DN, 1991. Prefrontostriatal connections in relation to cortical architectonic organization in rhesus monkeys. J. Comp. Neurol. 312, 43–67. [PubMed: 1744243]

Yeterian EH, Pandya DN, Tomaiuolo F, Petrides M, 2012. The cortical connectivity of the prefrontal cortex in the monkey brain. Cortex 48, 58–81. [PubMed: 21481342]

Zhang W, Luck SJ, 2011. The number and quality of representations in working memory. Psychol. Sci. 22, 1434–1441. [PubMed: 21987693]

Zhou QJ, Jiang ZZ, Ding JH, 2021. Reward Expectation Differentially Modulates Global and Local Spatial Working Memory Accuracy. Front. Psychol. 12.

Zink CF, Pagnoni G, Martin-Skurski ME, Chappelow JC, Berns GS, 2004. Human striatal responses to monetary reward depend on saliency. Neuron 42, 509–517. [PubMed: 15134646]

Zold CL, Hussain Shuler MG, 2015. Theta Oscillations in Visual Cortex Emerge with Experience to Convey Expected Reward Time and Experienced Reward Rate. J. Neurosci. 35, 9603–9614. [PubMed: 26134643]

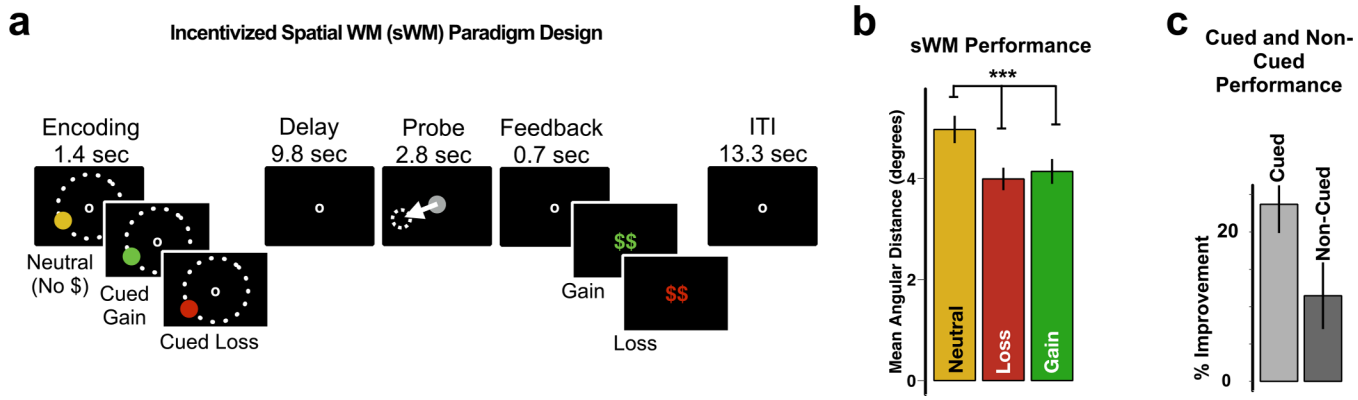

Fig. 1.

Motivated Spatial Working Memory Task Design and Behavioral Results. A. The task consisted of six blocks that tested spatial working memory and motivated spatial working memory. Each trial had a similar structure, and depicted are examples of neutral trials, cued reward and cued loss trials. In each trial, the encoding epoch referred to when the colored target circle appeared. During the delay epoch, participants maintained the spatial location after the colored target circle disappeared. During the probe epoch, participants used a high-precision joystick to move a gray circle to where they remembered the colored target circle had been presented. The measure of sWM accuracy was the angular distance between where the probe (gray circle) was placed and where the colored target circle had been originally presented. For cued incentive trials (shown), the color of the target circle at encoding signaled the incentive at stake. Green circles signaled the possibility to win money and red circles signaled the possibility to lose money. Cued incentive trials were accompanied by feedback about the amount of money won or lost on each trial. Across the full task there were a total of six blocks of 20 trials each: a motor block (without working memory); a baseline sWM block; 2 cued incentive blocks; 2 non-cued incentive blocks. The presentation of incentive blocks was counterbalanced across participants. See Supplemental Figure 1 and Methods for more details. B. There was a significant main effect of Incentive (neutral, gain, loss) ($F(2,64) = 12.62$, $p < 0.001$). Participants had better sWM performance (measured as angular distance (degrees) between the target circle presentation and the gray probe placement) in both gain (green) and loss (red) trials, compared to neutral, baseline sWM trials (yellow). See Results for full statistics. Error bars are standard error of the mean (SEM). C. There was a significant main effect of Cue (neutral, cued and non-cued) ($F(2,64) = 15.7$, $p < 0.001$). Graph depicts the percent improvement in sWM accuracy (angular distance, degrees) for cued and non-cued incentivized sWM trials, compared to the baseline, neutral sWM trials. Participants had better sWM performance in both types of incentivized trials, compared to the neutral sWM trials, and better performance in the cued incentive trials compared to the non-cued incentive trials. See Results for full statistics. Error bars are SEM.

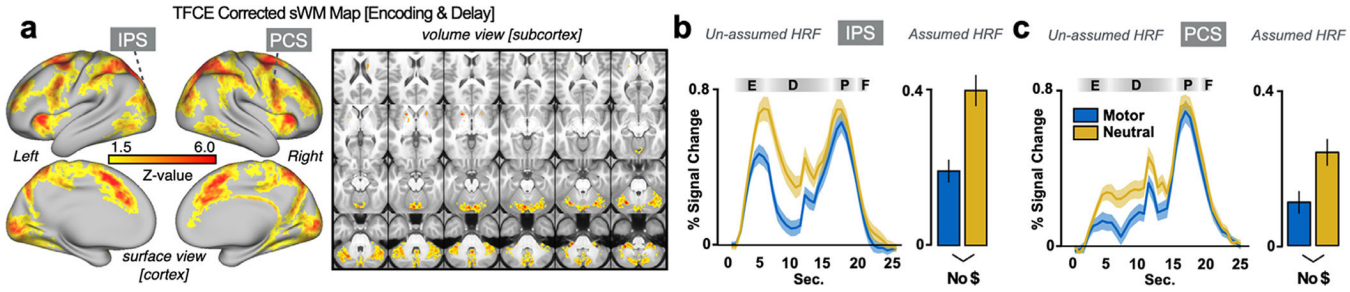

Fig. 2.

Brain-wide activation of sWM. A. Brain regions activated by the main effect of sWM (sWM > Motor, across encoding and delay epochs). The baseline, neutral sWM condition engaged brain regions well known to support working memory, including frontoparietal, striatal and cerebellar regions (main effect, $p < 0.05$, FWE-corrected, 5000 permutations). To identify clusters here and in subsequent whole-brain analyses, TFCE was applied. TFCE approaches cluster correction by calculating a weighted sum of a local cluster signal, thereby avoiding the need to arbitrarily set a cluster threshold for significance (Smith and Nichols, 2009). B. BOLD signal is illustrated from the left IPS, highlighted as this region has previously been shown to be critical for supporting sWM through topographic maps. On the left is the hemodynamic response constructed using an FIR model (unassumed response). The approximate windows of time during the encoding (E), delay (D), probe (P) and feedback (F) are highlighted at the top of the graph. The relative peak during the delay epoch represents participants pressing a button during a reminder for central fixation that was presented during all conditions (see methods). On the right is the plot of the BOLD signal from the left IPS using assumed HRF modeling. Bars are SEM. C. BOLD signal illustrated from the right PCS is also highlighted as this region is critical for supporting sWM. The hemodynamic response is on the left, and created using an FIR model (unassumed response). The approximate windows of time of encoding (E), delay (D), probe (P) and feedback (F) are highlighted at the top of the graph. On the right is the plot of the BOLD signal from the right PCS using assumed HRF modeling. Bars are SEM.

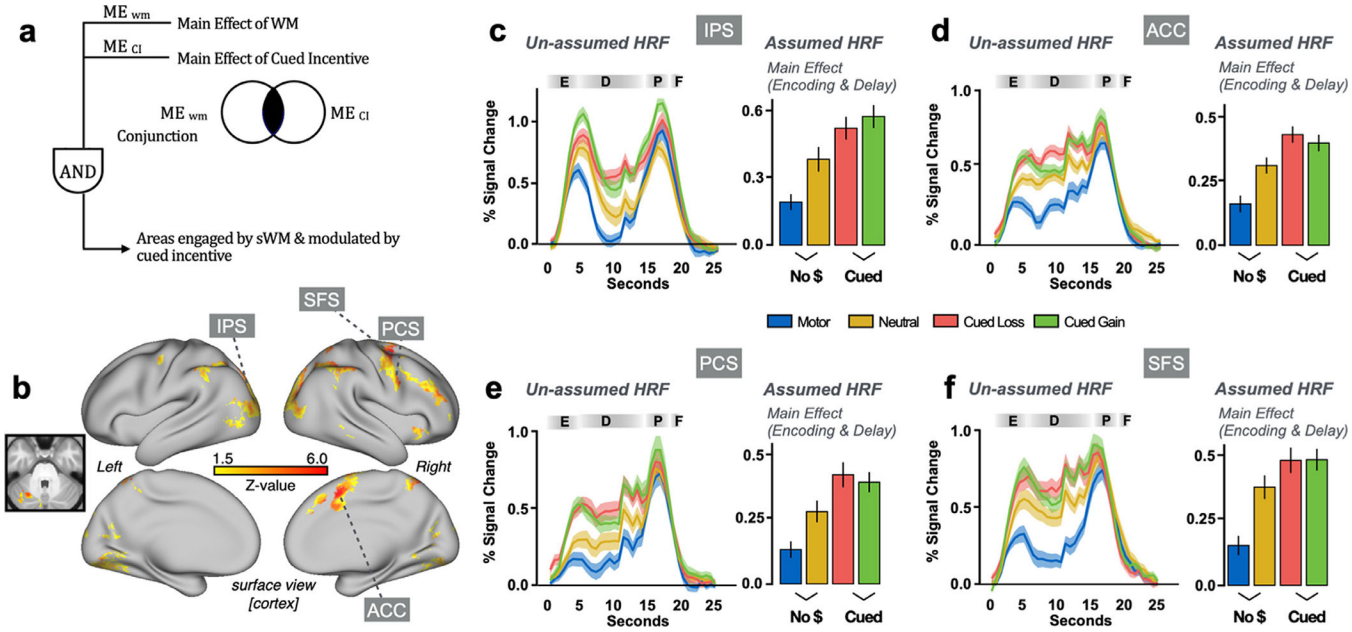

Fig. 3.

Main Effect of Cued Incentives on sWM Neural Circuits. A. A 2-way conjunction was applied to identify brain regions that supported sWM and were impacted by cued incentives across encoding and delay epochs (main effect). This conjunction involved the whole-brain corrected maps of the main effect of sWM and the main effect of Cued Incentive (neutral, cued gain and cued loss) (each $p < 0.05$, FWE-corrected, 5000 permutations prior to conjunction). B. The regions that remained were sWM regions that were modulated by cued incentives across epochs, and included prefrontal and parietal cortices, anterior cingulate cortex, insula cortex, and ventral occipitotemporal cortices. C. The BOLD signal timecourses for the left IPS are depicted during the motor (blue), baseline neutral sWM (yellow), cued gain (green) and cued loss (red) trials using an FIR model (left, unassumed response, envelopes are SEM). Overall there was elevated BOLD signal during cued gain and loss conditions, compared to the neutral sWM condition. The peak during the delay epoch reflects the reminder for central fixation that occurred in all conditions. The top legend shows the approximate windows of events (encoding (E), delay (D), probe (P) and feedback (F)). Illustration using an assumed HRF also showed that both cued gain and cued loss trials had elevated BOLD signal, compared to the neutral, baseline sWM trials (right, error bars are SEM). D. The BOLD signal timecourse in the right ACC is relatively elevated during the cued gain and cued loss conditions, compared to the neutral sWM condition (left, unassumed response, envelopes are SEM). The approximate time windows of events are at the top (encoding (E), delay (D), probe (P) and feedback (F)). Elevated BOLD signal during cued gain and cued loss conditions, compared to the neutral sWM condition, is illustrated on the right modeled with an assumed HRF (bars are SEM). E. For the right PCS, timecourses depicted using an FIR response showed elevated BOLD signal during the cued gain and loss conditions, compared to the neutral sWM condition (left, envelopes are SEM) (Encoding, Delay, Probe and Feedback time windows are displayed at the top). Elevated BOLD signal during the cued gain and loss conditions was also seen with an assumed response HRF (right, bars are SEM). F. In the superior frontal sulcus (SFS), elevated BOLD signal was

seen during the cued gain and loss conditions, compared to the neutral sWM condition, as illustrated with unassumed and assumed HRF modeling (left, right, respectively; envelope and error bars are SEM, trial epochs depicted at the top of the timecourses as with the other graphs).

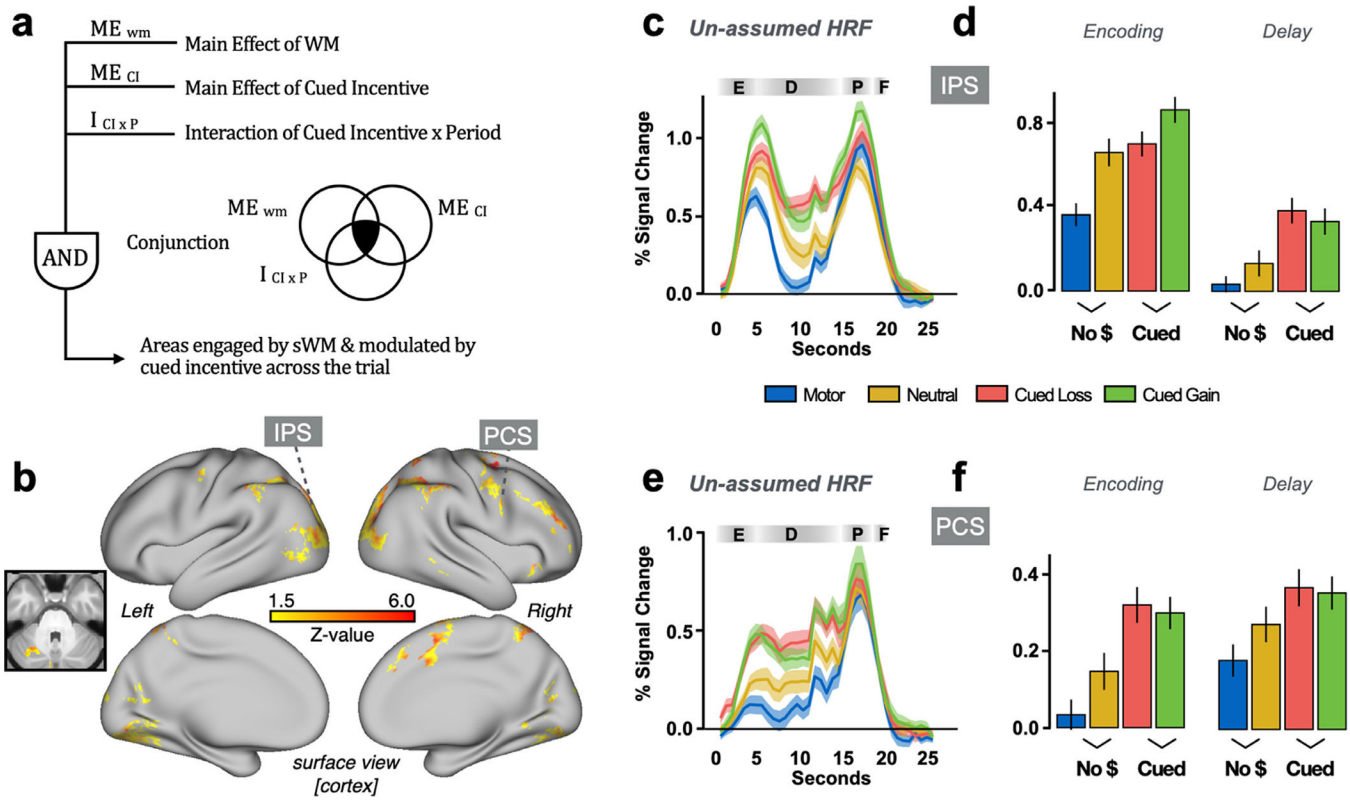

Fig. 4.

Interactive Effects of Cued Incentives on sWM Neural Circuits. A. A 3-way conjunction was applied to identify brain regions that support sWM and were impacted by cued incentives differentially during encoding and delay epochs. This conjunction consisted of the whole-brain corrected maps of the main effect of sWM, the main effect of Cued Incentive, and the interaction of Cued Incentive x Epoch (encoding vs delay) (each $p <$ 0.05, FWE-corrected, 5000 permutations prior to conjunction). B. The regions that remained were sWM regions that were modulated by cued incentives differentially during epochs, and included areas of the prefrontal cortex, parietal cortex, cingulate cortex, ventral temporal cortex and cerebellum. C. The BOLD signal timecourse is illustrated for the left IPS during motor (blue), baseline neutral sWM (yellow), cued gain (green) and cued loss (red) trials using an FIR model (unassumed response). Both cued gain and cued loss trials had elevated BOLD signal, compared to the neutral, baseline sWM trials. Envelopes are SEM. The peak during the delay epoch reflects the reminder for central fixation that occurred in all conditions. Approximate windows of event timings are depicted at the top (encoding (E), delay (D), probe (P) and feedback (F)). D. In the left IPS, the BOLD signal was extracted and illustrated using an assumed HRF within each epoch. During the encoding epoch (left), BOLD signal was elevated for the cued gain trials, though not the cued loss trials. During the delay epoch (right), BOLD signal was elevated for both the cued gain and loss conditions. Error bars are SEM. E. The reconstructed signal timecourse is illustrated in the right PCS, with windows approximating the timing of trial epochs at the top. Overall the BOLD signal was elevated in this region during encoding and delay for the cued gain and cued loss trials, compared to the neutral, baseline sWM condition. As with other illustrations

of the unassumed responses, the small peak during the delay epoch reflects the reminder for central fixation, which occurred during all conditions. Envelopes are SEM. F. The BOLD signal in the right PCS is illustrated using an assumed HRF. For encoding, illustration showed greater BOLD signal in cued gain and loss conditions, compared to the neutral, baseline sWM condition (left). This was similarly seen in the delay epoch (right). Error bars are SEM.

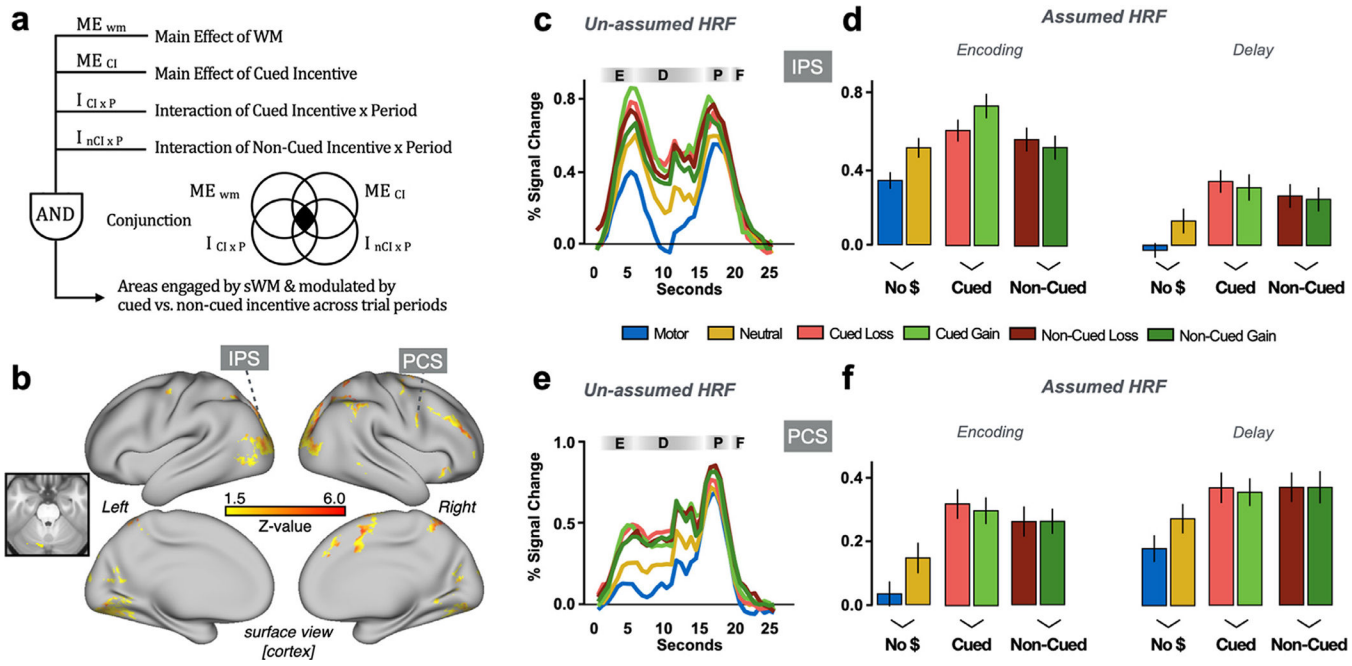

Fig. 5.

Effects of Non-Cued Incentives on sWM Neural Circuits. A. We tested whether non-cued incentive trials that relied on internal representation of incentives modulated sWM signals similarly to cued incentive trials. The whole-brain corrected interaction of Non-Cued Incentive (neutral, non-cued gain, and non-cued loss) x Epoch (encoding, delay) was conjuncted with the prior conjunction logic to create a four-way conjunction. B. Remaining areas following the four-way conjunction reflected sWM regions that were modulated by cued and non-cued incentives across epochs. These included relatively more restricted areas in the bilateral parietal, lateral occipital, and ventral temporal cortices, right PCS, right dlPFC, right ACC and cerebellum, compared to the prior three-way conjunction ($p < 0.05$, FWE-corrected, 5000 permutations). C. BOLD signal timecourses constructed using an FIR model (unassumed response) in the left IPS. Dark green and dark red lines refer to the non-cued gain and non-cued loss conditions, respectively. Approximate windows of trial epochs are depicted at the top (encoding (E), delay (D), probe (P) and feedback (F)). Both non-cued gain and non-cued loss BOLD signals were elevated, compared to the neutral sWM condition (yellow). The relative peak during the delay epoch reflects the participants receiving a reminder for central fixation and pressing a button in response. D. Assumed HRF modeling in the left IPS illustrated no difference between non-cued gain or non-cued loss and neutral sWM conditions during the encoding epoch (left). During the delay epoch there was elevated BOLD signal during the non-cued gain and non-cued loss conditions, compared to the neutral sWM condition (right). Error bars are SEM. E. In the right PCS, construction of the BOLD signal timecourse using FIR modeling (unassumed response) illustrated elevated BOLD signal during the encoding and delay epochs during non-cued gain (dark green) and non-cued loss (dark red) conditions (windows of trial epochs are depicted at the top as with other timecourses). F. In the right PCS, illustration of the assumed response HRF revealed greater BOLD signal during non-cued gain and non-cued loss conditions separately during both the encoding and delay epochs. Error bars are SEM.

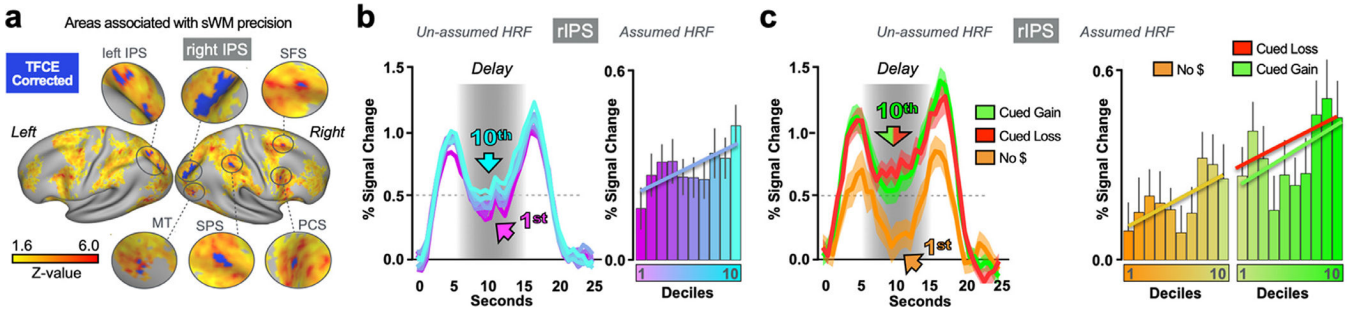

Fig. 6.

Trial-by-Trial BOLD Signal Changes Associated with Improvements in sWM. A. We regressed sWM performance (angular accuracy) for each trial with BOLD signal changes in each of the voxels of the sWM map (yellow). Within the sWM network, a subset of regions displayed greater trial-by-trial BOLD signal that was associated with better sWM performance across conditions (blue, $p < 0.05$, FWE-corrected, 5000 permutations). B. We directly illustrated the BOLD signal changes across all of the trials, as seen in the whole map findings (A). The sWM performance for each trial was binned into deciles within each participant. The deciles were entered as regressors in a GLM and the BOLD signal changes for each regressor were plotted across participants. The first decile refers to the decile with the worst performance, and the tenth decile refers to the decile with the best performance. On the left are unassumed BOLD signal responses constructed with an FIR response in the right IPS, and on the right are the BOLD signal responses illustrated with an assumed response model in the right IPS along with a linear trend line. There was greater BOLD signal in deciles with better sWM performance. The cyan blue color refers to the decile with the best performance (10th decile) and the magenta color refers to the decile with the worst performance (1st decile) across all trial types used for (A). The gradient between the two colors depicts deciles 2–9. Envelopes and error bars are SEM. C. Trial-by-trial BOLD signal changes associated with improvements in sWM performance were plotted for separate conditions using a similar binning approach for sWM performance. sWM performance was binned by decile within each participant and within each condition, then entered into a GLM, and results were plotted across subjects to illustrate BOLD signal changes related to sWM performance. On the left are unassumed BOLD signal responses for the decile with the best performance in the cued gain (green) and cued loss (red) conditions, and for the decile with the worst performance in the neutral sWM (orange) condition. Envelopes are SEM. On the right are illustrations of the assumed HRF responses for each decile within each participant and each condition along with a linear trend line. Elevated BOLD signal was seen with better performance within each condition, with overall elevated BOLD signal in the cued gain (green) and cued loss (red) conditions, compared to the neutral sWM (orange) condition. The trend line for the cued loss condition is shown in red. Error bars are SEM.

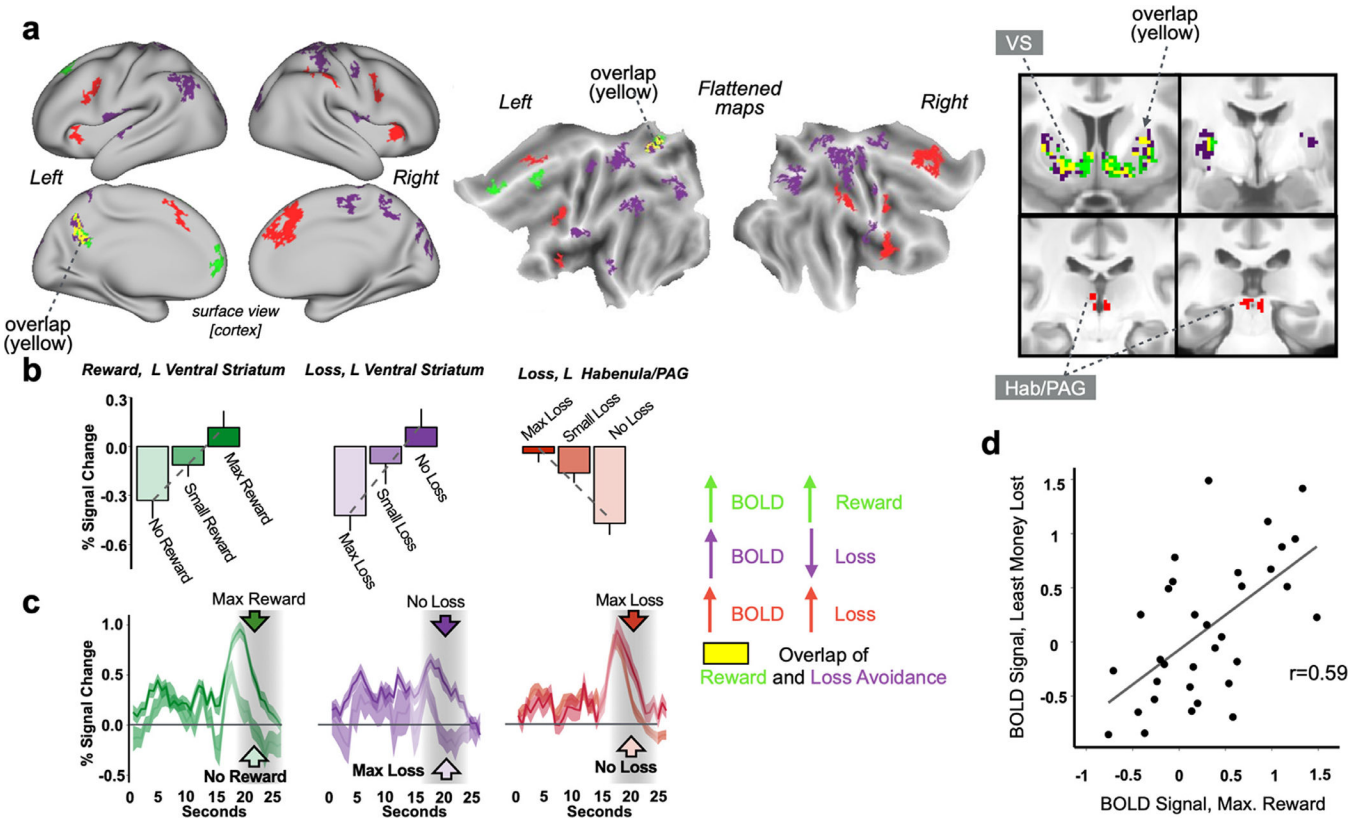

Fig. 7.

Trial-by-Trial Incentive Receipt Following sWM Performance. A. The amount of money won or lost in each cued incentive trial was regressed with the BOLD signal in each voxel of the brain ($p < 0.05$, FWE-corrected, 5000 permutations). Across the brain, regions where trial-by-trial increases in BOLD signal were associated with greater money won are depicted in green, regions where trial-by-trial increases in BOLD signal were associated with more money avoided in loss are in purple, and regions where trial-by-trial increases in BOLD signal were associated with more money lost are in red. Flattened cortical maps are in the center, with specific subcortical coronal views on the right. Note that regions where BOLD signal increases were associated with greater money won or greater money avoided in loss overlapped within the ventral striatum and precuneus (overlap depicted in yellow). B. Illustrations of the BOLD signal changes using an assumed HRF. The parametric amount of money won or lost in each trial within each participant was modeled in a GLM at the individual level, and plotted across subjects. Trial-by-trial increases in BOLD signal associated with increased money won was illustrated in the left ventral striatum (green). Trial-by-trial increases in BOLD signal associated with more money avoided in loss was illustrated in an overlapping region of the left ventral striatum (purple) and trial-by-trial increases in BOLD signal associated with more money lost was illustrated in a region straddling the left habenula and periaqueductal gray (PAG). Error bars are SEM, and the dashed lines represent a linear trend line. C. Unassumed HRF timecourses plotted using an FIR model for the greatest and smallest amount of incentive received for each incentive valence. Arrows are pointing at the approximate time of the feedback epoch. Envelopes are

SEM. D. Participants who had the greatest BOLD signal response to the highest amount of money won also had the greatest BOLD signal response to the greatest amount of money avoided in loss ($r = 0.59$, $p < 0.001$).